Optimizing an adult tacrolimus population pharmacokinetic model and extrapolating it to paediatric renal transplant recipients

Karoline Sandbakken

Master Thesis
Section for Pharmacology and Pharmaceutical Biosciences
45 credits

Department of Pharmacy
Faculty of Mathematics and Natural Sciences

UNIVERSITY OF OSLO

May 2023

Optimizing an adult tacrolimus population pharmacokinetic model and extrapolating it to paediatric renal transplant recipients

by

Karoline Sandbakken

Thesis for the degree of Master of Pharmacy
Section for Pharmacology and Pharmaceutical Biosciences

Department of Pharmacy
Faculty of Mathematics and Natural Sciences

UNIVERSITY OF OSLO

May 2023

Supervisor:
Professor Anders Åsberg
Section for Pharmacology and Pharmaceutical Biosciences, Department of Pharmacy, UiO

2023

Optimizing an adult tacrolimus population pharmacokinetic model and extrapolating it to paediatric renal transplant recipients

Karoline Sandbakken

http://www.duo.uio.no/

Printing: Reprosentralen, Universitetet i Oslo

Abstract

Introduction: Following organ transplantation there is a risk of the body rejecting the transplanted organ. To prevent this solid organ transplant recipients (SOTRs) are dependent on life-long immunosuppressive therapy. Tacrolimus is one of the drugs used as standard maintenance therapy following renal transplantation. The drug has a narrow therapeutic window and expresses large pharmacokinetic (PK) inter- and intrapatient variability. Therapeutic drug monitoring (TDM) of tacrolimus, used to optimize individual personalised dosage regimens, is mandatory for all SOTRs. Studies have proven that the use of population pharmacokinetic (PopPK) models to develop individual dosage regimens for tacrolimus increased the share of individuals with concentrations within the therapeutic window compared to standard TDM. Tacrolimus PopPK models have been presented for the paediatric population. However, the clinical use is limited and there is no data on successful extrapolation of an adult tacrolimus PopPK model to the paediatric population for which the adult model is valid. The aim of this thesis was to optimize a tacrolimus PopPK model used for adult renal transplant recipients and extrapolate it to paediatric renal transplant recipients to determine the lower limit of age for when the adult model is still valid.

Method: The modelling process consisted of improving an adult PopPK model and validating the extrapolation of the improved model to a paediatric population. Model development and validation was performed in the add-on package to R, Pmetrics, using a non-parametric mixed effects model. Both internal and external validation was performed on the models, and the improved adult models were tested for their performance with limited sampling strategies (LSS).

Results: The final improved model showed a better prediction of the maximum concentration (C_{max}). The model's performance when using a LSS was improved. When using a LSS the model provided slightly better prediction of the later times of the dosing interval for Prograf®, but tended to overestimate the C_{max}. The Improved model was not successfully extrapolated to the paediatric population. The lower limit of age for when the adult model is still valid in the paediatric population was not possible to determine.

Conclusion: The improvement of a PopPK model for tacrolimus resulted in a model with better performance when applied to a LSS for estimating the area under the plasma drug

concentration–time curve (AUC). The improved model was not successfully extrapolated to the paediatric population. There was no indication that the model's performance in the youngest patients was worse than in the older patients in the paediatric population. Further improvement of the model is necessary before it can be implemented in the clinic for paediatric patients.

Forord

Denne oppgaven ble utført ved seksjon for farmakologi og farmasøytisk biovitenskap, Farmasøytisk institutt, ved Universitetet i Oslo, under veiledning av professor Anders Åsberg.

Først og fremst vil jeg rette en stor takk til Anders for god hjelp og veiledning gjennom hele masteren. Det ble en stor omvelting da vi i slutten av høstsemesteret ikke lenger kunne gjennomføre den planlagte studien. Du var rask med å finne en ny oppgave, og har oppmuntret og støttet meg underveis. Takk for at du alltid har vært tilgjengelig og tatt deg tid til alle spørsmål. Og takk for gode råd og konstruktive tilbakemeldinger gjennom skriveprosessen.

Jeg vil også rette en stor takk til Markus Herberg Hovd for verdifull hjelp med R og Pmetrics. Du har gjort alt fra hjelpe med å utforme figurer til å ta deg tid på kvelder og i helger for å hjelpe meg med programmeringen da Pmetrics ikke ville samarbeide.

Takk til Stian for at du har tatt deg av stort og smått hjemme for å gjøre det siste halvåret lettere for meg. Din støtte og tålmodighet har vært viktig den siste tiden. Takk til Hilde for at du alltid bare har vært en telefonsamtale unna. Du tar deg alltid tid til å lytte, og har vært en stor støtte og motivasjon. Takk til mine studievenner som har gjort dette til fem flotte år, og en spesiell takk til Martine og Kristine. Studiehverdagen hadde ikke vært den samme uten dere. Til slutt vil jeg takke familien min for all kjærlighet og støtte i alt jeg gjør.

Oslo, mai 2023

Karoline Sandbakken

Table of contents

Abbreviations

%RMSE	Percent root mean squared error of prediction
AIC	Akaike information criterion
AUC	Area under the plasma drug concentration–time curve
BIC	Bayesian information criterion
BMI	Body mass index
BSA	Body surface area
C0	Trough concentration
CL	Clearance
CL/F	Apparent central clearance
C_{max}	Maximum concentration
CYP3A	Cytochrome P450 3A
F	Bioavailability
FFM	Fat-free mass
FKBP12	FK506 binding protein 12
k_a	Absorption rate constant
k_{el}	Elimination rate constant
LAM	Lambda used for the for the Heaviside step function
LSS	Limited sampling strategy
NPAG	Non-parametric Adaptive Grid
OP	Observed versus predicted

PK	Pharmacokinetics
PopPK	Population pharmacokinetic
Q/F	Intercompartmental clearance
R^2	Coefficient of determination
SAEs	Serious adverse events
SD	Standard deviation
SOTRs	Solid organ transplant recipients
$t_{1/2}$	Elimination half-life
TDM	Therapeutic drug monitoring
T_{lag}	Absorption lag time
T_{max}	Time to reach maximum concentration
TXT	Time after transplantation
V_d	Volume of distribution
V_d/F	Central volume of distribution
V_p/F	Apparent peripheral volume of distribution

1 Introduction

1.1 Renal transplantation

The first successful renal transplantation was performed in Boston in 1954 by Joseph Murray (1). The transplantation was performed in a 23-year-old man with progressive chronical renal failure, with his monozygotic twin as the donor. Prior to the transplantation the patient's condition had been maintained with periodic haemodialysis. The patient lived for 26 years following the transplantation without rejecting the graft and thereby became the first long-term survivor (2).

Two years later, Leif Efskind at the Oslo University Hospital, Rikshospitalet, led the first transplantation in Scandinavia using a kidney from an allogenic, ABO-incompatible donor. Whole body irradiation and cortisone were used as immunosuppression, and the patient lived for 30 days (3). Seven years later, in 1963, Ole Jacob Malm performed a transplantation at Oslo University Hospital, Ullevål. The donor was the mother of the patient, and the patient received azathioprine in combination with steroids for immunosuppression. The patient lived for 22 years. This was the first successful renal transplantation in Norway (3). Since 1983, all renal transplantations are now performed at Oslo University Hospital, Rikshospitalet (4).

1.1.1 Immunosuppressive therapy

To prevent the body from rejecting the transplanted organ, solid organ transplant recipients (SOTRs) are dependent on life-long immunosuppressive therapy (5, 6). Current immunosuppressive therapy has improved 1-year graft and patient survival, which is now over 96%, and reduced the number of rejection episodes following kidney transplantation to under 10% (6). In Norway, standard maintenance therapy after renal transplantation consists of calcineurin inhibitor (tacrolimus or ciclosporin), mycophenolic acid and glucocorticoid (prednisolone) (6, 7). Calcineurin inhibitors inhibits the activation of T cells by competitive binding to calcineurin (8, 9). Mycophenolic acid drugs inhibits the proliferation of both T and B cells by inhibiting inosine monophosphate dehydrogenase, which is involved in the de novo synthesis of guanine nucleotides (10). The inhibition of T and B cells weakens the immune system and response. Glucocorticoids inhibits the immune system by inducing anti-

inflammatory genes and suppressing expression of inflammatory transcription factors such as activator protein 1 and nuclear factor kappa-light-chain-enhancer of activated B cells (11).

Finding the right combination of these drugs for the patient to achieve adequate immunosuppression (to avoid rejection) and experience fewest possible side effects can be challenging as these drugs already in therapeutic doses induces a number of serious adverse events (SAEs) (6).

1.2 Tacrolimus

1.2.1 Mechanism of action

Tacrolimus (formerly known as FK506) is a calcineurin inhibitor that binds to the cytosolic immunophilin FK506 binding protein 12 (FKBP12) in T-cells (12, 13). The tacrolimus-FKBP12 complex inhibits calcineurin phosphatase activity by competitive binding to calcineurin which inhibits dephosphorylation and the activation of nuclear factor of activated T cells. This suppresses the transcription of the proinflammatory cytokines, such as interleukin-2, and thereby inhibits the activation of T cells (8, 12-14). The immunosuppression by tacrolimus prevents graft rejection (14).

1.2.2 Adverse events and toxicity

As calcineurin is not T cell specific the use of tacrolimus can give rise to toxicity and other SAEs (12). Tacrolimus has a narrow therapeutic window (15), and the risk of adverse events increases with increasing systemic exposure (16). However, patients might experience SAEs even within therapeutic doses (6, 16). SAEs of tacrolimus include nephrotoxicity, neurotoxicity, post transplanted diabetes mellitus, hypertension, infectious complications, and malignancies (16-18). Other common adverse events include hyperkalaemia, hypomagnesaemia (17, 18), tremor, insomnia, headache, diarrhoea and nausea (14).

1.2.3 Pharmacokinetics

Pharmacokinetics (PK) is the relationship between input and exposure following drug administration. It describes the drug concentration over a given period of time in conjunction with the amount of drug administered (systemic exposure–time profile), following absorption,

distribution, and elimination (10). Figure 1 shows a plasma drug concentration-time curve following administration of a single oral dose.

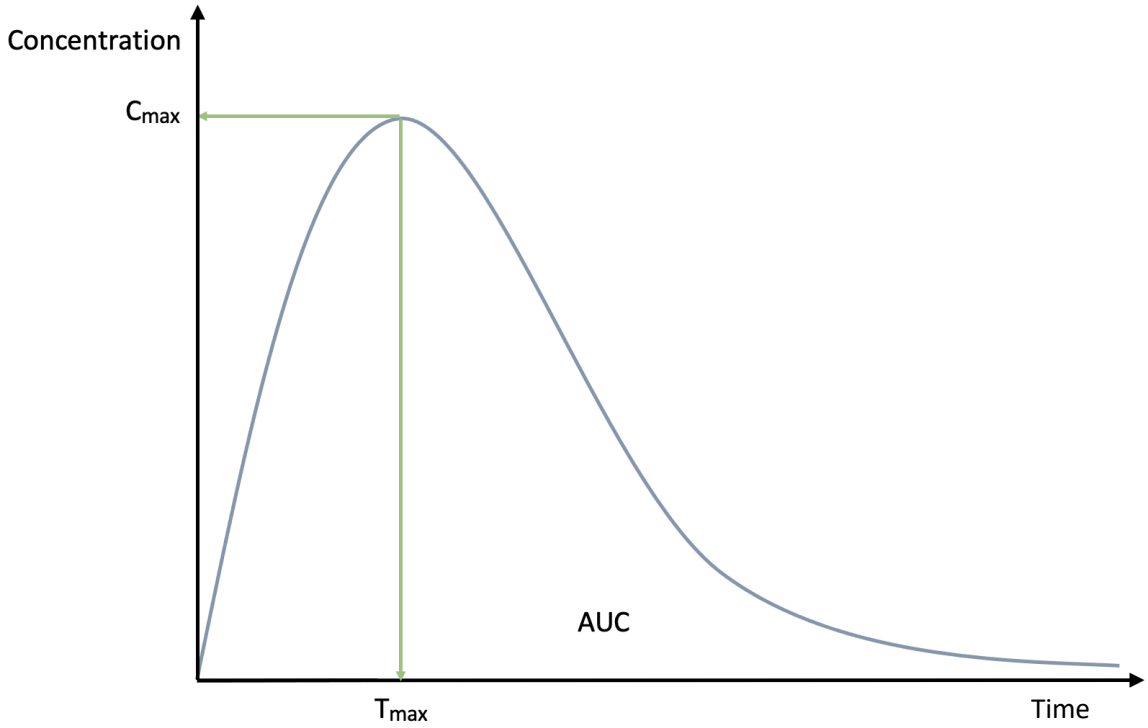

Figure 1. *The plasma drug concentration-time curve following a single oral dose of a drug portraying the time course of the plasma concentration, including maximum concentration (C_{max}), the time of which C_{max} occures (T_{max}) and the total systemic expousre of the drug, area under the plasma drug concentration-time curve (AUC).*

PK parameters describes absorption, distribution and elimination, and are used to describe the PK in a population. Table 1 describes central PK parameters and variables.

Table 1. *Central pharmacokinetic (PK) parameters and variables. PK parameters describes absorption, distribution and elimination of a drug. Primary PK parameters are parameters that are only affected by physiological variables, and not by changes in other PK parameters. Secondary PK parameters are affected by changes in other pharmacokinetic parameters and/or drug dose.*

Pharmacokinetic parameters	
Primary parameters	
Absorption rate constant (k_a)	Describes the rate at which a drug is absorbed from the site of administration and enters systemic circulation.
Bioavailability (F)	The fraction of the administered dose that reaches systemic circulation intact.
Volume of distribution (V_d)	A non-physiologic volume that describes the distribution of a drug in plasma and tissue compartments.
Clearance (CL)	The volume of plasma which is cleared of drug per unit of time.
Secondary parameters	
Elimination rate constant (k_{el})	The fraction of drug eliminated per unit of time.
Elimination half-life ($t_{1/2}$)	The time required for the concentration of the drug in the body to decrease by half.
Pharmacokinetic variables	
Area under the plasma drug concentration–time curve (AUC)	The cumulative systemic exposure of a drug for the given period of time.
Trough concentration (C0)	The drug concentration immediately before administration of the next dose.
Maximum concentration (C_{max})	The highest observed plasma drug concentration after administration.
Time to reach maximum concentration (T_{max})	The time after administration at which the highest plasma drug concentration is observed.

Tacrolimus expresses large PK inter- and intrapatient variability. The dose requirement can vary widely between patients, in addition to vary over time for each patient (18, 19). Following oral administration tacrolimus is absorbed rapidly in most patients. However, some patients have a slower and prolonged absorption. The oral bioavailability (F) ranges from 5-93% but is usually low with a mean of 25% (19). Tacrolimus' low F can be explained by the fact that the drug is a substrate of extensive first pass metabolism through cytochrome P450 3A (CYP3A) enzymes. In addition, absorbed tacrolimus is transported back to the

gastrointestinal lumen by P-glycoprotein, making the metabolism through CYP3A more efficient (18-20).

Tacrolimus binds broadly to erythrocytes, and the concentration of tacrolimus is on average 15 times higher in blood than in plasma. Approximately 99% is bound in plasma (18).

As mentioned, tacrolimus is a substrate of extensive first pass metabolism through CYP3A, the most important metabolizing enzymes being CYP3A4 and CYP3A5 (18, 21). The interpatient variability of CYP3A expression is substantial, and expression of CYP3A4 in liver can vary from 10- to 100-fold differences (18). As CYP3A5 expression is polymorphic, only carriers of the *CYP3A5 *1* allele express active CYP3A5 (21, 22). Carriers of the *CYP3A5 *1* allele have a higher metabolism of tacrolimus and may require a higher dose, on average 100% higher, compared to homozygous carriers (*CYP3A5*3/*3*) (21, 23, 24).

In addition to CYP3A variability, differences in haematocrit and albumin concentrations, concomitant diseases or administration of other drugs (18, 25), bodyweight (18, 26), and non-adherence (25) can also be causes of variability in tacrolimus PK.

Tacrolimus PK may also change over time after transplantation, often resulting in dosage reduction. This is generally believed to correlate with decreased tacrolimus clearance (CL) and possibly increased F following increased time post-transplantation (18). Studies have also found that reduction of prednisolone dose and changes in haematocrit and albumin might contribute to this (18, 27).

Prednisolone is a CYP3A inducer. As tacrolimus is a substrate of extensive first pass metabolism through CYP3A concurrent intake of prednisolone will likely increase tacrolimus CL and increase the dose requirement. The CYP induction might also reduce tacrolimus F due to increased first pass metabolism. In accordance with time after transplantation the dose of prednisolone is reduced, and thus the patients' dosage requirement will likely be reduced (27, 28).

Although only the unbound fraction of the drug is pharmacologically active, the concentration of tacrolimus is measured as total concentrations in whole blood, including both unbound and bound tacrolimus. As tacrolimus binds extensively to erythrocytes, high values of haematocrit and albumin increase the amount of bound tacrolimus and may lead to an increased measured tacrolimus whole blood concentration without an increased therapeutic effect as the unbound

concentration remains unchanged (18, 29, 30). Haematocrit increases extensively following kidney transplantation. This makes haematocrit an important covariate to consider when interpreting tacrolimus data, especially during the early posttransplant period (27, 29). However, the use is not widespread in the clinic.

1.2.4 Pharmacokinetic properties in the paediatric population

Children are not just "little adults", and so the PK of tacrolimus in the paediatric population differs from that of the adult population (18, 24, 31). It has been reported that children have a similar F to adults, but a higher volume of distribution (V_d) and CL (32-34). In addition, the paediatric population have a greater proportion of intrapatient variability than adults. Children does not have a linear relationship between weight and CL of tacrolimus (24, 32).

Allometric scaling is a mathematical concept that describes how different physiological properties change in proportion to change in body size (35). It is commonly used when extrapolating a population model to a paediatric population to adjust for differences in body size between adults and children (36). In population pharmacokinetic (PopPK) modelling allometric scaling is used to adjust PK parameters to an appropriate body size measure.

In paediatric PK studies it is common for the population to have a much wider relative range in body size than adults. CL and V_d are parameters that are normally functions of body size. Thus, if they are not scaled their influence on the model may be masked by the effect of body size (36). In general, children have a higher CL and V_d of drugs compared to adults. This also goes for tacrolimus (32-34). However, the relationship of CL and weight for tacrolimus in children is not linear (24, 32), and as allometric scaling to body size assumes that CL is proportional to body size this might not be an optimal solution for tacrolimus.

1.2.5 Therapeutic drug monitoring of tacrolimus

Therapeutic drug monitoring (TDM) is measuring the concentration of specific drugs at predefined time intervals and using it to optimize individual personalised dosage regimens (37). For tacrolimus the trough concentration (C0) is measured in whole blood frequently after transplantation. The patient's dose is then adjusted according to measured dose compared to target dose (38), with the patients individual characteristics as age, weight and genotype taken in to consideration (39). As tacrolimus has a narrow therapeutic window and

high inter- and intrapatient PK variability, TDM is mandatory for all SOTRs (40, 41). The recommendation of TDM of tacrolimus is rationalized by the correlation between tacrolimus blood concentration, primarily C0, and clinical outcomes (42, 43), and is strongly recommended by a large number of studies (42).

1.3 Population pharmacokinetic modelling

1.3.1 Population pharmacokinetics

To analyse pharmacokinetic data both non-compartmental and compartmental analysis are relevant to use. Non-compartmental analysis is a simple method for evaluating key PK parameters and patient variability. The method does not rely on assumptions of the underlying model, is quick and can easily be automated. However, when only sparse data are available the method comes to short (44). Sparse data refers to data only containing C0 measurements, whilst rich data refers to data with drug concentration measurements drawn at least six to eight times during the same dose interval.

Compartmental analysis is based on the body being divided into compartments, with the number of compartments being dependent on the number of exponential terms needed to describe the plasma concentration–time data. The model describes transportation rates and drug concentrations within the compartments which is result of mass transport, i.e., distribution between the compartments. Combined with associated covariates, a compartmental model can provide a greater insight into the data and improved predictability (45). Figure 2 shows an example of a two-compartment model for a drug.

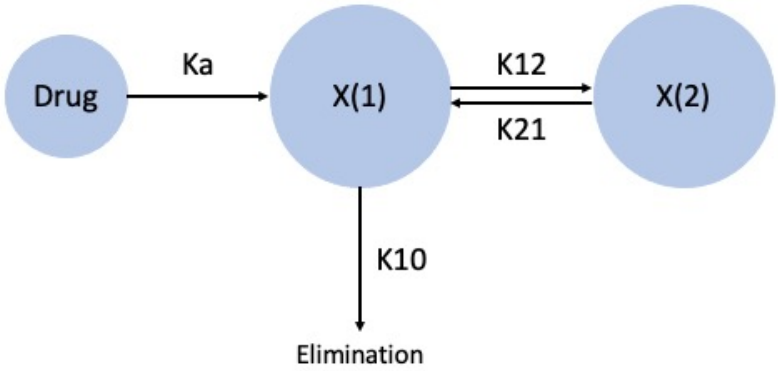

Figure 2. *A two-compartment model of a drug. The absorbed drug enters compartment one (X(1)). From X(1) the drug is either distributed to compartment two (X(2)) or eliminated from the compartment (K10). Ka, absorption rate constant; X(1), compartment one; K10, rate constant of elimination; K12, transfer rate constant from compartment one to compartment two; K21, transfer rate constant from compartment two to compartment one; X(2), compartment two.*

PopPK models use drug concentrations and covariates from multiple individuals within a population to describe the time course of drug exposure and inter- and intrapatient variability. PopPK can be used even with sparse data and does not require a strictly timed sampling schedule, as long as the exact dose- and sampling times are known (46-48). In addition, information of previous dosing intervals can be included to improve model predictions for the individual patients (48).

In drug development, PopPK models have high utility in predicting PK aspects of drug candidates and is a useful tool in designing dosage recommendations. In the clinic, PopPK models can provide guidelines for individualised dosing based on population PK derived Bayesian estimates (49) that uses observed data to update the prior information in the model (48, 50, 51). The observed data are blood concentrations collected from the patient, often combined with other patient specific data as age or body weight, and the prior data is the distribution of PK parameters of a similar population of that to be studied (48).

PopPK models can be based on either parametric or nonparametric methods. Parametric models assume that the population parameters come from a specified probability distribution described by other single-valued parameters as measures of central tendency, standard deviation or covariances. The parameter distribution is assumed to be the same for the whole population and is often normal or lognormal (47, 52). Parametric models can separate interpatient variability from intrapatient variability, but are not great for achieving a realistic description of populations that does not fit the model assumptions of distribution (52).

Unlike parametric models, nonparametric models make no assumptions about the model parameter distribution (47, 53). This gives the model the ability to detect unanticipated outliers and subpopulations (47, 54). Nonparametric models are superior to parametric models in providing the distribution of parameter values for the population that has the highest probability of matching the true distribution, as illustrated in Figure 3. The statistical properties of nonparametric models make them relevant for designing precise individual dosage regimens (53). However, unlike parametric models, nonparametric models do not have the ability to separate interindividual variability from intraindividual variability (52).

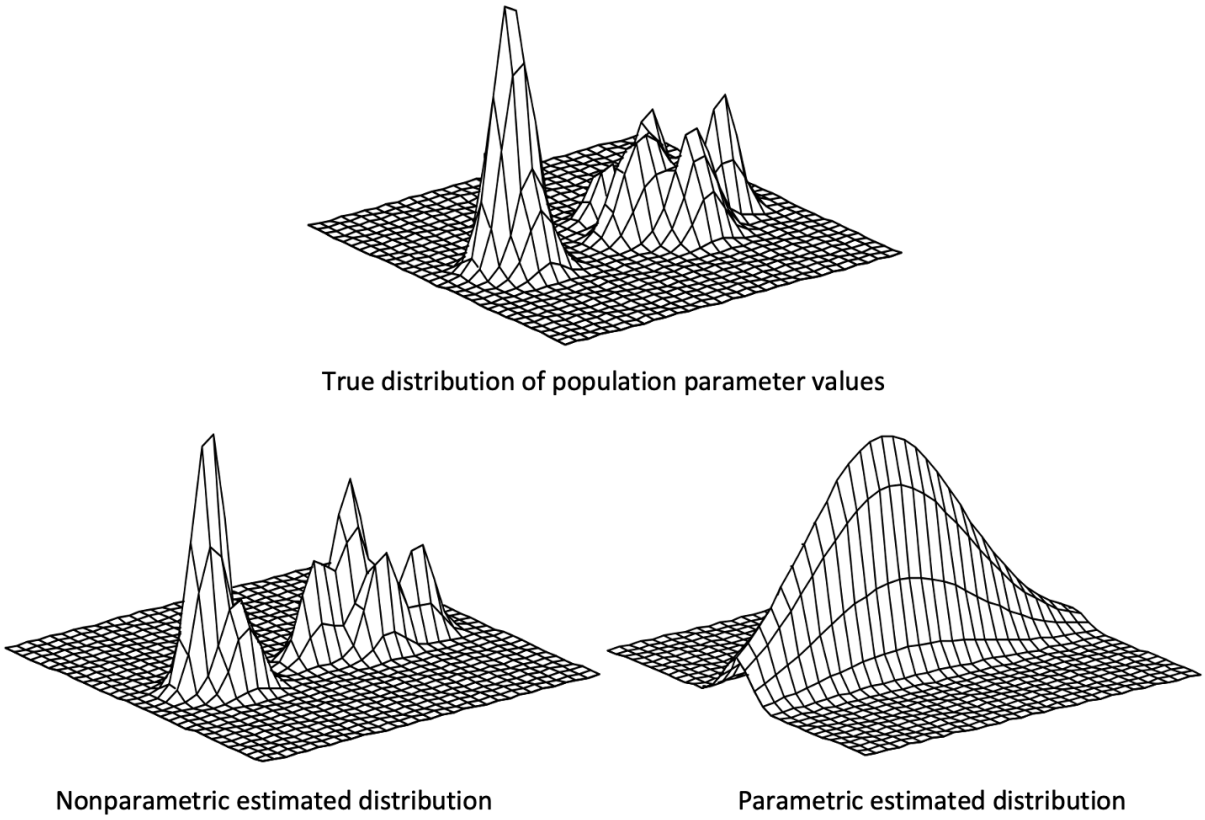

Figure 3. *Illustration of true, nonparametric estimated and parametric estimated distribution of population parameter values in a population of non-normal distribution. Adapted from Jelliffe et al. (52).*

1.3.2 Pmetrics

Pmetrics is an add-on package to R, a programming language and software for statistical computing and graphics (55), designed for pharmacometric researchers. The package is used to perform non-parametric and parametric population pharmacokinetic modelling and simulation.

To estimate a distribution of the population parameters with the highest probability of accuracy Pmetrics creates a non-parametric mixed effects model using a calculation method called Non-parametric Adaptive Grid (NPAG) written in Fortran. The model created by NPAG consists of sets of discrete estimates for all parameters in the model with associated probabilities. Each set of estimates constitutes a support point. Each subject in the study population can be explained by several support points, but the total amount of support points cannot exceed the total number of subjects (47, 54).

NPAG determines the maximum likelihood matrix given the observed data provided, such as the measured drug concentration and drug dose, by searching for the most likely parameter values in a grid (47). A given number of grid points, based on the number of parameters in the model, are evenly distributed in the grid (54). However, this can be overruled by the user. Pmetrics then estimates probability values for each grid points. For each search low-probability points are removed, and new grid points are added around the high-probability points that were not removed, called support grid points, before initiating a new search (47), as illustrated in Figure 4. When the increment in the maximum likelihood algorithms value in the last two cycles approaches 0, convergence is reached. When a predefined criterion for convergence is reached, the repetition of removing and adding grid points will cease. This implies that the parameter values of highest probability are found (47, 56, 57).

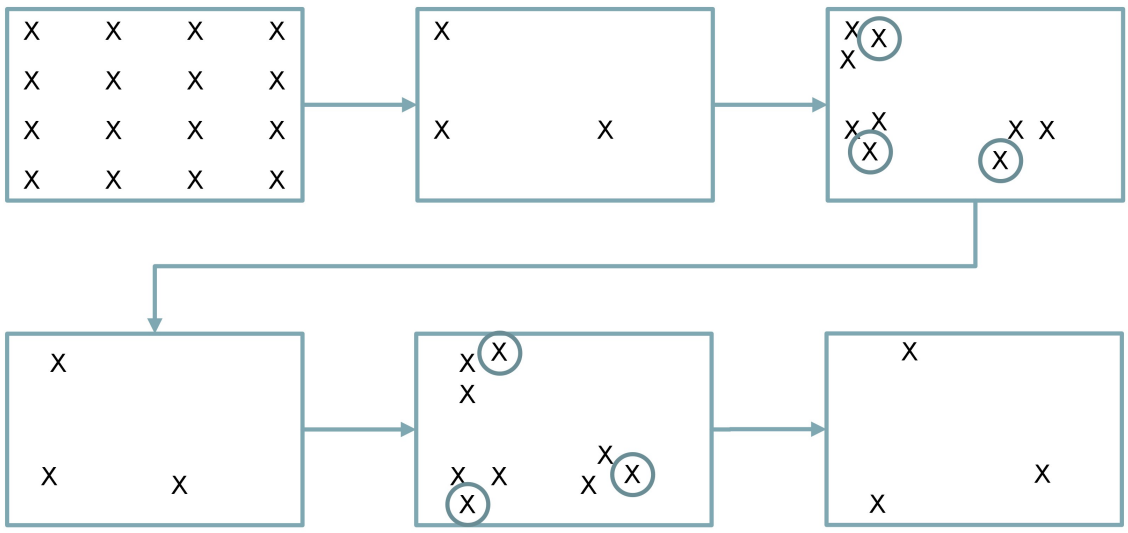

Figure 4. *Illustration of nonparametric adaptive grid. X represents the support points, and the circled X are the support points with the highest probability. Pmetrics calculates the probability of the support points in the grid. The low-probability points are removed, and only the points with the highest probability remains as support points. New support points are added around the remaining support points, and Pmetrics calculates the new probabilities. The iterating continues until Pmetrics have found the parameter values of highest probability, and convergence is reached.*

Mixed effects model is a statistical model that includes random effects, which include pharmacokinetic parameters such as CL and V_d, and fixed effects which is an error model. The error model consists of two components representing the analytical error and extra process noise. The analytical error is described by standard deviation (SD). SD is estimated by the third-degree polynomial equation:

$$SD = C_0 + C_1 \cdot obs + C_2 \cdot obs^2 + C_3 \cdot obs^3$$

where *obs* is the observed concentration, obs^2 is the observed concentration squared, obs^3 is the observed concentration cubed, and the coefficients C_0, C_1, C_2 and C_3 are determined from analytical error in the local laboratory and fixed in the model (54, 58). A gamma or lambda function is included to describe additional process noise related to the observations and not a result of the analytical technique:

$$Error = SD \cdot gamma$$

or

$$Error = \sqrt{SD \cdot lambda^2}$$

The gamma function is multiplicative, and the lambda function is additive. Low gamma and lambda values that approximate 1 are considered high quality data (54, 58).

As a minimum, a model file and a data file are required for Pmetrics to run NPAG. The data file is a comma-separated file (.csv). It must contain fixed patient data such as identification, dose, and serum concentrations as a minimum, and may also contain covariates, such as demographic data, genotypes and organ function. The model file is a text file containing information about the structural components of the model such as primary and secondary variables, covariates, differential equations and the error model (54).

When a nonparametric run is performed, NPAG will search for optimal values within the intervals for the random parameter values set by the developer in the model file. Numerous combinations of different parameter boundaries are to be tested for each model contender to find the optimal estimated parameter values. Each time a change is made the model must be run again, making model development a time-consuming process.

1.3.3 Tacrolimus population pharmacokinetic models

Numerous PopPK models have been developed for tacrolimus (15). Previous studies have proven that the use of PopPK models to develop individual dosage regimens for tacrolimus increased the share of individuals with concentrations within the therapeutic window compared to standard TDM (38, 59). As tacrolimus PK parameter values tend to differ in

patients dependent on type of organ transplantation, PopPK models are often developed for a given population based on type of organ transplantation (18).

Tacrolimus PopPK models have been presented for the paediatric population for different types of organ transplantation (60-82). However, the clinical use is limited. Several studies suggested that the starting dose of tacrolimus in renal transplants should be higher in patients with a lower bodyweight (62, 73, 74, 82) and CYP3A5-expressers (62, 69, 73, 74, 82). There is no data on successful extrapolation of an adult tacrolimus PopPK model to the paediatric population and the lower limit of age for which the adult model is valid.

1.4 Aim of the study

PopPK models are essential tools in adapting individual tacrolimus treatment. However, the clinical use of PopPK models in the paediatric population is limited and there is a lack of data on extrapolation of adult models to paediatric patients. The aim of this thesis was to optimize a tacrolimus PopPK model used for adult renal transplant recipients and extrapolate it to paediatric renal transplant recipients to determine the lower limit of age for when the adult model is still valid.

2 Materials and methods

2.1 Computer hardware and software

Due to the time-consuming process of running models and minor troubles with the software, the model development and validation were run on three computers, at times in parallel on two of them. Information about the computers used in this master's thesis is presented in Table 2.

The models were run using the add-on package Pmetrics (version 1.9.7) in the software R (version 4.1.2). The development environment RStudio (version 2021.9.2.382) was used when running R. For internal validation and creating plots, the add-on packages Tidyverse (version 2.0.0) and ggplot2 (version 3.4.2) were used.

***Table 2**. Information about the processor, memory, and operating system of the computers used for model development and validation. Three different computers were used.*

	Processor	**Memory (RAM)**	**Operating System**
Main computer: MacBook Pro	1.4 GHz Quad-Core Intel Core i5	8 GB	Apple macOS Ventura, Version 13.2
Second computer: ASUS ZenBook	2.3 GHz Intel Core i5-8300H	16 GB	Windows 10 Home, Version 22H2
Third computer: MacBook Pro	2.3 GHz Quad-Core Intel Core i5	8 GB	Apple macOS Ventura, Version 13.2.1

RAM, random-access memory.

2.2 Population data

The data used for model development, validation and extrapolation was obtained from adult and paediatric patients who underwent organ transplantation at Oslo University Hospital, Rikshospitalet, during the periods of 2011-2018 (40, 83-86) and 2013-2021 (87) respectively. The adult population data consisted of data from 136 patients from five clinical studies, ranging in age from 21 to 79 years (40, 83-86). The data was randomly split into two datasets: Development dataset consisting of 92 patients used for model development, and Validation dataset consisting of the remaining 44 patients used for external validation.

The paediatric patient data was obtained from the PedTac study, which began in 2013 with the aim of developing a PopPK model for personalized dosing of tacrolimus in paediatric transplant patients. Data from 64 patients, ranging in age from eight months to 18 years, was used. Of this 43 patients' data were from renal transplantation, 17 from liver transplantation, and 4 from combined renal and liver transplantation. The data included information from early after transplantation, other hospitalization episodes, and annual follow-ups (87).

All patients provided written informed consent for their data to be used in PopPK modelling, with patients younger than 16 years having their consent signed by next of kin.

2.2.1 Preparation of the paediatric dataset

The paediatric dataset contained both sparse and rich data. Some patients had registered observations of dosing and concentrations of up to a year. However, the observations came at large intervals, and there were more observations of doses than concentration measurements. For the Improved model to run on the dataset, the dataset had to be reduced to containing fewer observations. To datasets where made: one containing all observations, including sparse data, for each patient from 0 to 48 hours named the Paediatric dataset, and one containing only data with at least two tacrolimus measurements per dose interval named the Rich paediatric dataset.

The paediatric population used four formulas of tacrolimus: Prograf®, dissolved Prograf®, Modigraf® and Advagraf®. As dissolved Prograf® and Modigraf® display similar properties as Prograf®, they were handled as Prograf® in the dataset.

2.3 Model development

Overall, the modelling process consisted of two main tasks. The first was to improve an adult PopPK model, hereby referred to as the New model, and the second was to extrapolate the improved model to work on the paediatric population. The New model originated from a previously developed model (88), hereby referred to as the Intermediate model. This is an improved model from the model currently in use at the clinic (89), hereby referred to as the Old model. The models are further described in sections 2.3.3-2.3.5.

The models were run in Pmetrics to estimate the distribution of the population parameters with the highest probability of accuracy. To do this, Pmetrics use a non-parametric mixed effects model; NPAG. NPAG is run by using the command NPrun(). After the run is completed, Pmetrics creates a R datafile containing several Pmetrics data objects. Pmetrics requires a model file and a data file to run NPAG.

2.3.1 Model file

The model file is a text file (.txt) containing information about the structural components of the model. It contains up to 11 blocks, where each block is marked by a hashtag (#) and a header. The models used in this master thesis contained the blocks #PRI, #COV, #SEC, #DIF, #F, #INI, #OUT and #ERR, as further described in Table 3. The order of the blocks is not important. However, the order of the covariates listed in #COV needs to be in the exact order of that in the input file.

Table 3. *Structural components of the model files used in this master's thesis. The model file consists of blocks, each marked by a hashtag (#) and a header consisting of capital letters.*

Header	Description
#PRI	Primary variables: model parameters that are to be estimated by Pmetrics or as fixed parameters with user specified values.
#COV	Covariates: subject specific data as specified in the input file, e.g., sex, weight, or haematocrit.
#SEC	Secondary variables: defined by equations that are combinations of primary variables and covariates, or other secondary variables.
#DIF	Differential equations: describing inputs and outputs of each compartment.
#F	Bioavailability: used to specify the bioavailability term
#INI	Initial conditions: used to specify the amounts in different compartments at time 0.
#OUT	Outputs: The tacrolimus concentration
#ERR	Error: describes the structure of the error model.

2.3.2 Data file

The data file is a comma-separated file (.csv). It must as a minimum contain fixed patient data, being the first 12 columns, and may also contain additional columns with covariates.

The order, capitalization, and names of the header of the fixed data are as presented in Table 4.

Table 4. *Description of the fixed patient data in the data file showing the fixed order, capitalization, and names of the header.*

Header	Description
#ID	A set of numbers or characters that identifies each individual.
EVID	Indicates type of event: 0 = observation; 1 = input; 4 = reset and input, all compartment values and time counter are reset to 0.
TIME	Elapsed time since the first event. The time is given in decimal hours.
DUR	The duration of an infusion. The duration is given in hours.
DOSE	The dose amount.
ADDL	The number of additional doses during interval II.
II	The interdose interval.
INPUT	Defines which input "DOSE" corresponds to.
OUT	The observation, e.g., measured concentration.
OUTEQ	Output equation number that corresponds to the "OUT" value, defined in the model file.
C0, C1, C2, C3	The coefficients for the assay error polynomial for that observation.

In addition to the fixed columns, the data file can also contain additional columns describing covariates such as demographic data, genotypes, and organ function. There are no requirements for the header names or order of the covariates, except that the order must be the same as in the model file. Figure 5 shows an extract of the data file used for model development.

POPDATA DEC_11																													
#ID	EVID	TIME	DUR	DOSE	ADDL	II	INPUT	OUT	OUTEQ	C0	C1	C2	C3	IC	STU	STER	M0F1	WTKG	HT	FFMES	TXT	HCT	AGE	CYP	ASY	FORM	BMI	BSA	TDOSE
22	1	0	0	3000	.	12	1	.	.	0.20205004	0.00431939	0.00060245	0	7.91	10	15	0	68.4	182	52.25	22	34	59	0	4	1	20.65	1.88	0
22	0	0.5	.	.	.	.	.	7.25	1	0.20205004	0.00431939	0.00060245	0	.	10	15	0	68.4	182	52.25	22	34	59	0	4	1	20.65	1.88	.
22	0	1	.	.	.	.	.	12.76	1	0.20205004	0.00431939	0.00060245	0	.	10	15	0	68.4	182	52.25	22	34	59	0	4	1	20.65	1.88	.
22	0	1.5	.	.	.	.	.	17.31	1	0.20205004	0.00431939	0.00060245	0	.	10	15	0	68.4	182	52.25	22	34	59	0	4	1	20.65	1.88	.
22	0	2	.	.	.	.	.	17.39	1	0.20205004	0.00431939	0.00060245	0	.	10	15	0	68.4	182	52.25	22	34	59	0	4	1	20.65	1.88	.
22	0	2.6	.	.	.	.	.	17.27	1	0.20205004	0.00431939	0.00060245	0	.	10	15	0	68.4	182	52.25	22	34	59	0	4	1	20.65	1.88	.
22	0	3	.	.	.	.	.	13.72	1	0.20205004	0.00431939	0.00060245	0	.	10	15	0	68.4	182	52.25	22	34	59	0	4	1	20.65	1.88	.
22	0	4	.	.	.	.	.	12.61	1	0.20205004	0.00431939	0.00060245	0	.	10	15	0	68.4	182	52.25	22	34	59	0	4	1	20.65	1.88	.
22	0	6	.	.	.	.	.	9.64	1	0.20205004	0.00431939	0.00060245	0	.	10	15	0	68.4	182	52.25	22	34	59	0	4	1	20.65	1.88	.
22	0	7	.	.	.	.	.	9.05	1	0.20205004	0.00431939	0.00060245	0	.	10	15	0	68.4	182	52.25	22	34	59	0	4	1	20.65	1.88	.
22	0	8	.	.	.	.	.	8.7	1	0.20205004	0.00431939	0.00060245	0	.	10	15	0	68.4	182	52.25	22	34	59	0	4	1	20.65	1.88	.
22	0	9	.	.	.	.	.	8.38	1	0.20205004	0.00431939	0.00060245	0	.	10	15	0	68.4	182	52.25	22	34	59	0	4	1	20.65	1.88	.
22	0	10.1	.	.	.	.	.	8.49	1	0.20205004	0.00431939	0.00060245	0	.	10	15	0	68.4	182	52.25	22	34	59	0	4	1	20.65	1.88	.
22	0	12.3	.	.	.	.	.	7.33	1	0.20205004	0.00431939	0.00060245	0	.	10	15	0	68.4	182	52.25	22	34	59	0	4	1	20.65	1.88	.
22	1	12.5	0	3000	.	12	1	.	.	0.20205004	0.00431939	0.00060245	0	.	10	15	0	68.4	182	52.25	22	34	59	0	4	1	20.65	1.88	12.5
22	1	24	0	3000	.	12	1	.	.	0.20205004	0.00431939	0.00060245	0	.	10	15	0	68.4	182	52.25	22	34	59	0	4	1	20.65	1.88	24

Figure 5. *Extract of the data file used for model development.*

2.3.3 Old model

The Old model is the model currently in use at the clinic (89). The model was a three-compartment model with absorption lag time (T_{lag}) and first order tacrolimus absorption. It was parameterized with apparent central clearance (CL/F), intercompartmental clearance (Q/F), central volume of distribution (V_d/F) and apparent peripheral volume of distribution (V_p/F). Variation in T_{lag} was described by time after transplantation (TXT) and fat-free mass (FFM). Haematocrit described variability in CL/F, Q/F, V_d/F and V_P/F. CL/F, Q/F and V_p/F were allometrically scaled to FFM, and V_p/F was allometrically scaled to body mass index (BMI). FFM was calculated by using the formula:

$$Males: \qquad FFM = \frac{WT \cdot 9270}{6680 + (216 \cdot BMI)}$$

$$Females: \quad FFM = \frac{WT \cdot 9270}{8780 + (244 \cdot BMI)}$$

where *FFM* is fat-free mass in kg, *WT* is weight in kg and *BMI* is body mass index in kg/m^2. The covariates included in the model were weight, height, sex, TXT, haematocrit, and steady state concentration. The error model included a lambda function.

The Old model was based on data from 69 patients. During model development it was run on the Development dataset containing new rich data to see if it would improve the performance of the model.

2.3.4 Intermediate model

The Intermediate model is a model previously developed from the Old model (88). The model was adjusted to haematocrit and allometrically scaled to body surface area (BSA), calculated by the Du Bois formula (90). CYP3A5 genotype was added as a covariate and, in addition to TXT, used to describe CL/F. F was described by CYP3A5 genotype, TXT and type of tacrolimus formulation. T_{lag} was described by TXT and tacrolimus formulation. The absorption rate constant (k_a) was described by type of tacrolimus formulation. FFM was calculated using a formula developed in renal transplant patients (91):

$$Males: \qquad FFM = \frac{11.4 \cdot WT}{81.3 + WT} \cdot (1 + HGT \cdot 0.052) \cdot (1 - Age \cdot 0.0007)$$

$$Females: \quad FFM = \frac{10.2 \cdot WT}{81.3 + WT} \cdot (1 + HGT \cdot 0.052) \cdot (1 - Age \cdot 0.0007)$$

FFM is fat-free mass in kg, *WT* is weight in kg, *HGT* is height in cm and *Age* is in years.

The covariates included in the model were number to identify the study the patient participated in, steroid dose, sex, weight, height, FFM, TXT, haematocrit, age, CYP3A5 genotype, bioanalytical method, rich or not rich data, known or not known exact time of tacrolimus dosing and sampling, type of tacrolimus formulation, BMI, and BSA. The error model included a gamma function.

2.3.5 New model

Before the start of this master's thesis, the Intermediate model was further developed to the New model. The New model was a five-compartmental model, as shown in Figure 6.

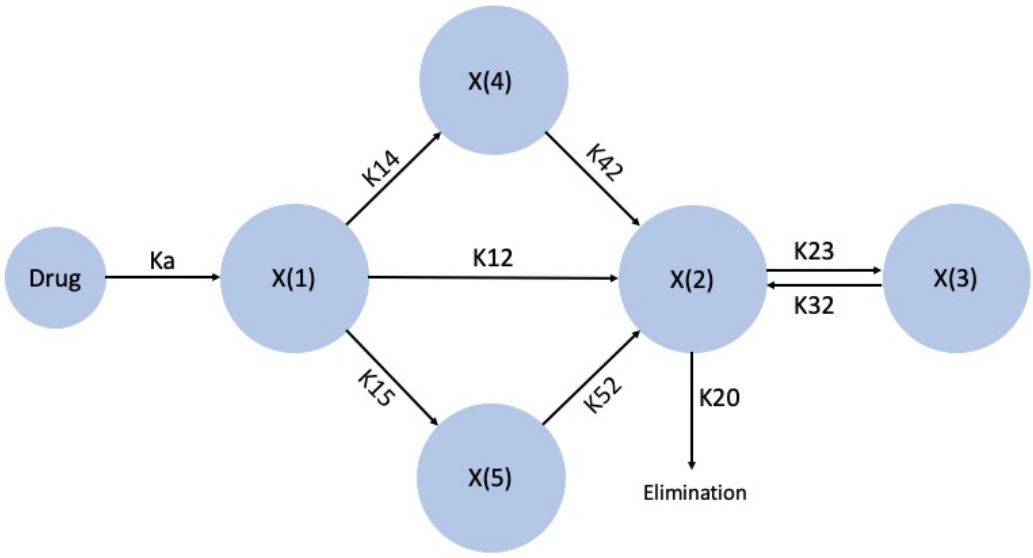

Figure 6. *A five-compartment model of tacrolimus. The model has to extra lag-compartments (X(4) and X(5)) to accord for the delayed absorption of Advagraf®. The absorbed drug first enters compartment one (X(1)). From X(1) Prograf® is transferred to compartment two (X(2)). Advagraf® is distributed between X(2), X(4) and X(5). The drug distributed to X(4) and X(5) is further transferred to X(2). From X(2) the drug is either distributed to compartment three (X(3)) or eliminated. X(1), compartment one; X(2), compartment two; X(3), compartment three; X(4), compartment four (lag-compartment for Advagraf®); X(5), compartment five (lag-compartment for Advagraf®); Ka, absorption rate constant; K12, transfer rate constant from compartment one to compartment two; K14, transfer rate constant from compartment one to compartment four; K15, transfer rate constant from compartment one to compartment five; K42, transfer rate constant from compartment four to compartment two; K52, transfer rate constant from compartment five to compartment two; K23, transfer rate constant from compartment two to compartment three; K32, transfer rate constant from compartment three to compartment two; K20, rate constant of elimination.*

It included the Heaviside step function (*H(t)*) instead of lag time. The Heaviside step function is a useful mathematical tool that allows for the modelling of sudden changes in a system. It is defined by

$$H(t) = 0\ for\ t < 0\ and\ H(t) = 1\ for\ t \geq 0$$

It appears only for a limited time period and vanishes outside this interval. It has no derivative at 0, and it's not continuous (92).

The Heaviside step function was added to depict the process of absorption in a realistic physiological manner. It was included in the description of the absorption from compartment 1 to compartment 2, and the delayed absorption from compartments 4 and 5 to compartment 2. Lambda was included in the function to create a gradual transition between the compartments. Lambda used for the Heaviside step function is hereby referred to as LAM to distinguish it from lambda used in the error model. LAM controls the amount of smoothing in the model. A larger value of LAM will result in a steep curve that resembles the use of lag time, while a smaller value of LAM will result in a flatter curve.

The Heaviside step function is coded in Fortran and included in the model as

$$K_{a,b} = Ka \cdot \left[\frac{1}{2} \cdot \left(1 + tan^{-1}\left(LAM \cdot (T - TDOSE - Tlag_a)\right) \cdot \frac{2}{\pi}\right)\right]$$

where $K_{a,b}$ is the limited time period for which the function appears, e.g., between compartment 1 and 2, Ka is the absorption rate constant of tacrolimus, LAM is the function of lambda, T is the relative time since the first dose of the patient, $TDOSE$ is the time of the dose relative to first dose, and $Tlag_a$ is the absorption lag time.

Type of tacrolimus formulation was used to describe T_{las}, k_a and intercompartment rate constants. F was described by formulation type and CYP3A5 genotype. V_d/F and differential equations for compartments 2 and 3 were allometrically scaled to BSA. The model was adjusted for haematocrit. All the covariates in the New model are presented in Table 5. The error model included a lambda function. The complete model files for the Old model, Intermediate model and New model are provided in Appendixes A-C.

Table 5. *Description of the covariates in the New model.*

Header	Description
IC	Initial condition. The measured trough concentration (C0) of tacrolimus. Equivalent to the steady-state concentration in the Old model.
STU	The study the patient participated in, identified by a number.
STER	Steroid dose in mg.
M0F1	Sex of the patient. Male = 0, Female = 1.
WTKG	Weight in kilograms.
HT	Height in cm.
FFFMES	Fat-free mass in kg.
TXT	Time after transplantation in days.
HCT	Haematocrit in percent.
AGE	Age in years.
CYP	CYP3A5 genotype. 1 = CYP3A5 expresser, 0 = CYP3A5 non-expresser.
ASY	Bioanalytical method.
FORM	Formulation of tacrolimus. 1 = Prograf®, 2 = Advagraf®.
BMI	Body mass index in kg/m^2.
BSA	Body surface area in m^2.
TDOSE	Time of dose administration relative to the first dose.

2.3.6 Improvement of the New model

The completed New model was the starting point of this master's thesis. Testing of the model had shown that it was unstable when using data based on limited sampling strategy (LSS). To improve this, different values of LAM were tested. In the New model LAM was set to "0.1, 100". This means that for each patient the model will search for a value of LAM with a lower bound of 0.1 and an upper bound of 100. To improve the model different single values of LAM between 2 to 30 were tested. To do this LAM was set as a numeric value followed by "!", and each value were tested on its own using the NPrun() command.

The values of LAM that gave the best results were further tested for their performance when using a LSS and by external validation. The model that had the best results overall from internal validation, external validation and a LSS ended up as the final Improved model and was used for further analysis and extrapolation.

2.4 Model validation

Model validation is a crucial step in PopPK modelling that involves assessing the accuracy and reliability of the model to ensure that it is fit for its intended purpose, such as making predictions in new patients (93). This is essential when selecting between multiple model candidates.

Model validation allows for internal and external validation. Internal validation assesses the model's performance on the same data used in the model development process, while external validation predicts response values for a new and unknown dataset. External validation provides a more realistic estimate of the model's performance on a new cohort of patients. This helps to ensure that the model is not overfitting to the data used during model development and can be used to make predictions for new data. External validation is crucial when developing population pharmacokinetic models used as dose adjustment tools in a clinical setting (94).

Model validation is a repetitive process that involves refining the model until an acceptable level of accuracy and reliability is achieved. This process may involve modifying the model structure, adding or removing covariates, or adjusting model parameters.

2.4.1 Internal validation

Internal validation was performed on each model after a run through the Development data. The percent root mean squared error of prediction (%RMSE), population and individual observed versus predicted (OP) plots, coefficient of determination (R^2), weighted residuals plot by time and concentration, Akaike information criterion (AIC) and Bayesian information criterion (BIC) were used in combination for internal validation of the models. In addition, individual time-concentration plots were investigated. %RMSE was the main validation metric, and decreased values of the metric weighted the most in the validation process in, supplemented with R^2 and individual time-concentration plots. The PMcompare() command in Pmetrics was used to compare models.

2.4.2 External validation

For external validation, the models were run with the Validation dataset, with the respective model as prior and no cycling. %RMSE, population and individual OP plots and R^2 were examined for each model after the run.

In addition, all the models were tested for their performance when using a LSS. The data used for LSS was from the Validation dataset. For the Old model, the best sampling times for LSS have been shown to be at 0, 1 and 3 hours after dosing for Prograf®, and so these times have also been used for Advagraf®. These sampling times were used for testing all the models, including when testing all the models with altered LAM during model improvement.

The final Improved model was further tested with different sampling times for LSS, with cycling applied, to find the optimal sampling times for both Prograf® and Advagraf®. From previous studies different sampling times for LSS have been suggested for tacrolimus. The studies suggest different compositions of sampling times from 0, 1, 2, 3, 4 and 5 hours after dosing (95-99). Based on this, different compositions of three sampling times between 0 and 6 hours after dosing were tested. The model was first tested on sampling times that were the same for Prograf® and Advagraf®. Then the dataset was split in two, one for Prograf® and one for Advagraf®. The split datasets were tested individually with several compositions of sampling times to find the optimal sampling times for each formulation. Then the sampling times proven best for each formulation were tested with the combined dataset.

For runs with a LSS the %RMSE for the predicted (LSS) versus observed (Validation dataset) area under the plasma drug concentration–time curve (AUC) was calculated. AUC was calculated using the logarithmic trapezoidal rule on the simulated data using all measured concentrations for each individual.

2.5 Extrapolation of the Improved model to the paediatric population

The Improved model was run on the Paediatric dataset and the Rich paediatric dataset with no cycling. %RMSE, population and individual OP plots, R^2 and plots of predictive error against age were examined. The model was also run on the Rich paediatric dataset without allometric

scaling to BSA to see how this would affect the results. This was done by changing BSA in the dataset to the same value used in the model file to centralize the parameter.

3 Results

3.1 Population demographics

3.1.1 Adult population

Patient demographics for the adult population are provided in Table 6. The patient population mostly consisted of males who were non-expressers of CYP3A5 and using Prograf®. The average age of the patients was 52 years for the development dataset and 53 years for the validation dataset. The average dose of tacrolimus and prednisolone for both datasets were 3.5 mg and 10 mg, respectively. The average number of tacrolimus concentration samples per patient was 11 for both datasets. TXT differed from 12 days to 16 years. Overall, the patient demographics were similar for the Development dataset and Validation dataset.

Table 6. *Demographics of the patients in the datasets used for development and validation of the adult models. Development dataset describes the demographics of the patients in the dataset used for development. Validation dataset describes the demographics of the patients in the dataset used for validation. The numbers show the average ± standard deviation unless otherwise stated.*

	Development dataset	Validation dataset
Patients (n)	92	44
Age (years)	52 ± 14	53 ± 14
Males (%)	79.3	79.5
Weight (kg)	79.5 ± 15.5	80.1 ± 15.8
Height (cm)	177 ± 9	176 ± 8
BMI (kg/m^2)†	25.4 ± 4.2	25.7 ± 4.3
BSA (m^2)‡	1.96 ± 0.21	1.96 ± 0.21
FFM (kg)§	53.9 ± 8.3	54.0 ± 8.4
Haematocrit (%)	38 ± 4	37 ± 4
CYP3A5 expresser (%)	13.02	18.2
Time after transplantation (days) (range)	540 (12, 3254)	531 (15, 5827)
Tacrolimus formulation (Prograf®/Advagraf®) (n)	60/32	33/11
Trough concentration (µg/L)	5.8 ± 1.7	6.1 ± 1.9
Tacrolimus dose (mg) (range)	3.5 (1, 15)	3.5 (1, 10)
Tacrolimus concentration samples (n per patient)	11 ± 2	11 ± 2
Prednisolone dose (mg) (range)	10 (2.5, 20)	10 (5, 15)

BMI, body mass index; BSA, body surface area; FFM, fat-free mass; CYP3A5, cytochrome P450 3A5; † BMI was calculated by dividing body weight (kg) on the squared height (m^2); ‡ BSA was calculated by using the Du Bois formula (90); § Fat-free mass was calculated by using a formula developed in renal transplant patients (91).

3.1.2 Paediatric population

Patient demographics for the paediatric population at time of the first dose are provided in Table 7. The paediatric population was more evenly distributed between both sexes than the adult population. The average age of the patients was 11 years in both datasets. Most of the patients were non-expressers of CYP3A5. The average dose of tacrolimus and prednisolone was slightly higher in the Paediatric dataset. TXT differed from 7 days to 16 years in the Paediatric dataset and 7 days to 15.5 years in the Rich paediatric dataset.

Table 7. *Demographics of the patients in the datasets used for extrapolation to the paediatric population. The Paediatric dataset included all observations from time 0 to 48 hours. The Rich paediatric dataset contained only data with at least two tacrolimus measurements per dose interval. The numbers show the average ± standard deviation unless otherwise stated.*

	Paediatric dataset	**Rich paediatric dataset**
Patients (n)	108	79
Age (years)	11 ± 5	11 ± 5
Males (%)	55.6	51.9
Weight (kg)	43.3 ± 21.7	41.1 ± 21.5
Height (cm)	140 ± 29	137 ± 28
BMI (kg/m^2)†	20.5 ± 6.0	20.3 ± 6.3
BSA (m^2)‡	1.28 ± 0.45	1.23 ± 0.44
FFM (kg)§	31.0 ± 14.9	29.3 ± 14.6
Haematocrit (%)	36 ± 5	36 ± 4
CYP3A5 expresser (%)	13.0	16.5
Time after transplantation (days) (range)	1821 (7, 5949)	1802 (7, 5673)
Trough concentration (µg/L)	5.1 ± 2.2	5.0 ± 2.4
Tacrolimus dose (mg) (range)	3.5 (0.35, 12)	3.0 (0.35, 12)
Tacrolimus concentration samples (n per patient)	2 ± 1	2 ± 1
Dose events (n per patient)	1	1
Prednisolone dose (mg) (range)	5.0 (0, 30)	3.5 (0, 20)

BMI, body mass index; BSA, body surface area; FFM, fat-free mass; CYP3A5, cytochrome P450 3A5; † BMI was calculated by dividing body weight (kg) on the squared height (m^2); ‡ BSA was calculated by using the Du Bois formula (90); § Fat-free mass was calculated by using a formula developed in renal transplant patients (91).

3.2 Model development

3.2.1 Old model

The Old model had a %RMSE of 19.3. When run on the new Development dataset %RMSE decreased to 6.7. AIC and BIC also decreased as shown in Table 8.

Table 8. *Results from the Old model and the Old model run on the Development dataset containing new rich data.*

	Old model	**Old model, new data**
%RMSE	19.3	6.7
R^2	0.94	0.99
AIC	3008	2999
BIC	3184	3053

%RMSE, percent root mean squared error of prediction; R^2, coefficient of determination; AIC, Akaike information criterion; BIC, Bayesian information criterion.

Figure 7 shows population and individual OP-plots for the Old model (upper row) and the Old model run on new data (lower row). R^2 of the individual OP-plot increased when the Old model was run on new data. However, R^2 of the population OP-plot decreased.

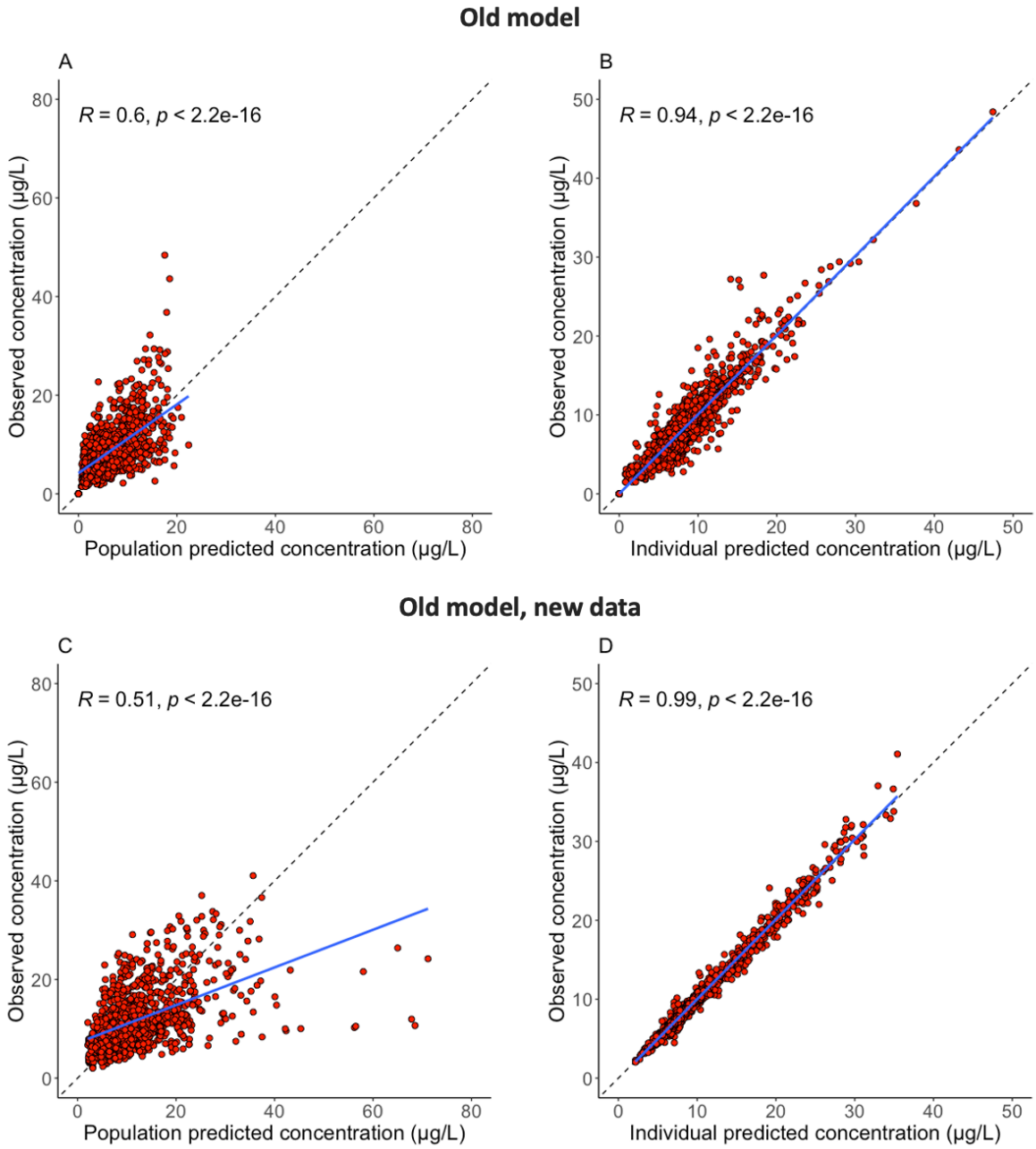

Figure 7. *Population (A) and individual (B) observed versus predicted (OP) plots for the Old model and population (C) and individual (D) OP plots for the Old model run on new data. R, coefficient of determination; p, probability.*

3.2.2 New model

For the New model %RMSE was 5.7, R^2 was 0.99, AIC was 2126 and BIC was 2214. %RMSE was decreased compared to the Old model. Figure 8 shows population and individual OP-plots for the New model. R^2 of the individual OP-plot increased for the New model compared to the Old model, but was the same as for the Old model run on new data.

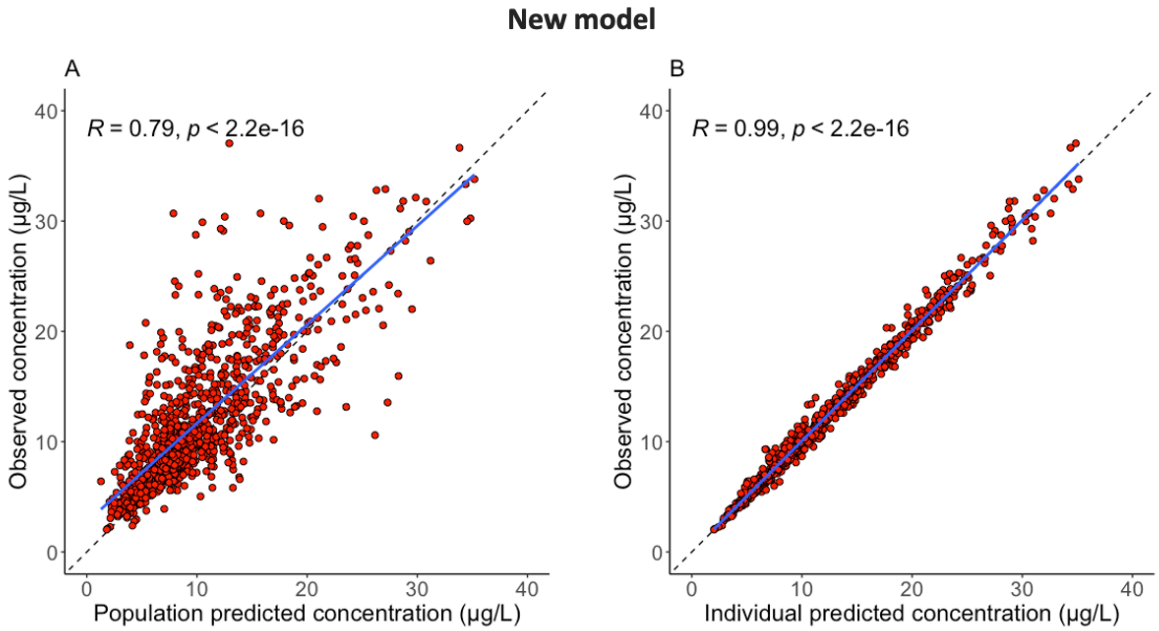

Figure 8. *Population (A) and individual (B) observed versus predicted plots for the New model. R, coefficient of determination; p, probability.*

3.2.3 Improvement of the New model

The New model was tested with different values of LAM between 2 to 30. The results of the runs are provided in Table 9.

Table 9. *Results from model development of the New model with different values of lambda for the Heaviside step function. The table is arranged in ascending order from lowest to highest %RMSE.*

LAM	%RMSE	R^2	AIC	BIC
22!	6.1	0.99	2571	2853
23!	6.5	0.99	2734	2817
18!	6.6	0.99	2794	2877
20!	6.6	0.99	2777	2860
30!	6.7	0.99	2742	2825
17!	6.7	0.99	2785	2868
19!	6.7	0.99	2853	2936
13!	6.7	0.99	2844	2927
26!	6.7	0.99	2743	2826
27!	6.7	0.99	2731	2814
16!	6.8	0.99	2803	2886
29!	6.8	0.99	2811	2894
12!	6.9	0.99	2889	2972
21!	6.9	0.99	2857	2941
28!	6.9	0.99	2793	2876
14!	7.1	0.99	2845	2928
9!	7.3	0.99	3008	3091
8!	7.8	0.99	3058	3141
11!	7.8	0.99	3215	3298
7!	8.1	0.99	3215	3298
6!	8.4	0.99	3216	3299
5!	8.8	0.99	3339	3422
10!	9.5	0.98	3527	3610
25!	9.7	0.98	3569	3652
24!	9.8	0.98	3554	3637
15!	10.1	0.98	3554	3637
4!	10.3	0.98	3731	3814
3!	10.5	0.98	3766	3849
2!	12.9	0.97	4177	4260

LAM, lambda used for the Heaviside step function; %RMSE, percent root mean squared error of prediction; R2, coefficient of determination; AIC, Akaike information criterion; BIC, Bayesian information criterion.

The values of LAM that gave the lowest %RMSE and AIC were “17!”, “18!”, “20!”, “22!”, “23!” and “30!”. These models, in addition to two models with a lower value of LAM (“9!”

and “13!”), were tested for their performance with a LSS with sampling times 0, 1, and 3 hours after dosing, and external validation. Table 10 shows the result of these validation runs. The value of LAM that gave the best results overall on internal validation, external validation and with a LSS was “22!”. This is the final Improved model, and this was used further in the current analyses.

Table 10. *Results from the models with the best values of lambda for the Heaviside step function for external validation on the Validation dataset and with limited sampling strategy with sampling times 0, 1 and 3 hours after dosing.*

	Validation dataset		LSS	
LAM	**%RMSE**	**R^2**	**Sample times**	**%RMSE AUC**
9!	15.7	0.96	0, 1, 3	12.3
13!	17.7	0.96	0, 1, 3	10.9
17!	19.7	0.96	0, 1, 3	11.5
18!	19.3	0.96	0, 1, 3	10.6
20!	18.2	0.96	0, 1, 3	35.0
22!	16.1	0.96	0, 1, 3	10.2
23!	15.9	0.96	0, 1, 3	25.9

Sample times are in hours after dosing. LSS, limited sampling strategy; LAM, lambda used for the Heaviside step function; %RMSE, percent root mean squared error of prediction; R2, coefficient of determination; AUC, area under the plasma drug concentration–time curve.

3.2.4 Final Improved model

In the final Improved model lambda was set to “22!”. The model converged after 8865 cycles to 66 support points. %RMSE was 6.1, R^2 was 0.99, AIC was 2571 and BIC was 2853. AIC and BIC were increased from the New model. The result from the final Improved model is presented in Table 11 compared to the results of the Old model and the New model. %RMSE was decreased compared to the Old model and slightly increased compared to the New model. R^2 was same as for the New model but decreased from the Old model.

Table 11. *Results from the Improved model compared to the Old model and the New model.*

	Old model	**New model**	**Improved model**
%RMSE	19.4	5.7	6.1
R^2	0.94	0.99	0.99

%RMSE, percent root mean squared error of prediction; R^2, coefficient of determination.

Figure 9 shows population and individual OP-plots for the Improved model. The individual OP-plot presents a good outcome of R^2 at 0.99. The population OP-plot displays a lower R^2 at 0.82.

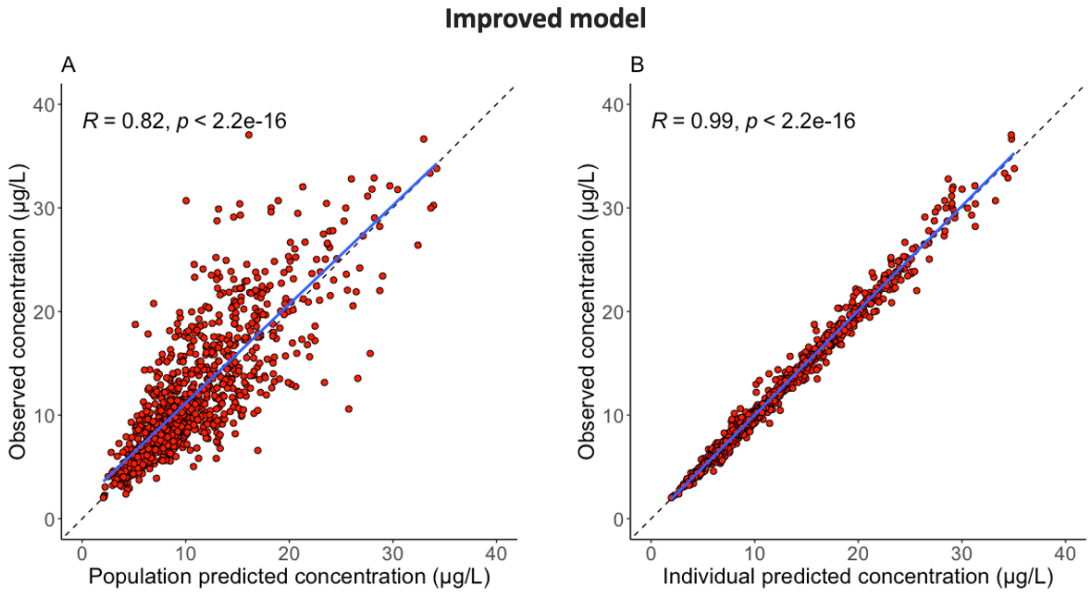

Figure 9. *Population (A) and individual (B) observed versus predicted plots for the Improved model. R, coefficient of determination; p, probability.*

Figure 10 shows the distribution of weighted prediction error for time after dosing and for concentrations for the Improved model. The plot for prediction error by time shows linearity but has outliers at the beginning of the time course and non-constant variance. The plot for prediction error by concentration also shows linearity and several outliers at high concentrations. Both plots show some over- and underestimation made by the model, particularly at lower time courses and higher concentrations.

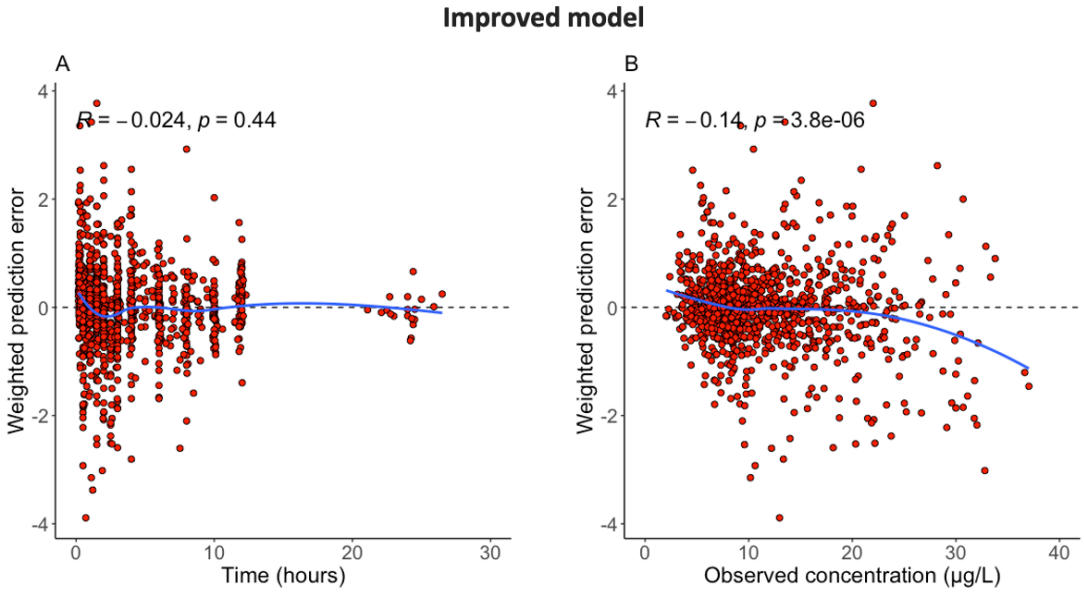

Figure 10. *Distribution of weighted prediction error for time after dose (A) and for concentrations (B) for the Improved model. R, coefficient of determination; p, probability.*

Figure 11 shows individual time-concentration plots for three individuals from the Development dataset for Prograf®, and Figure 12 shows the plots for Advagraf®. For both figures the plots at the upper row are from the Old model run on the Development dataset and the plots on the lower row are from the Improved model. The Old model tends to underestimate the predictions of the maximum concentration (C_{max}). The Improved model shows improvement in the prediction of the concentrations compared to the Old model for both formulations.

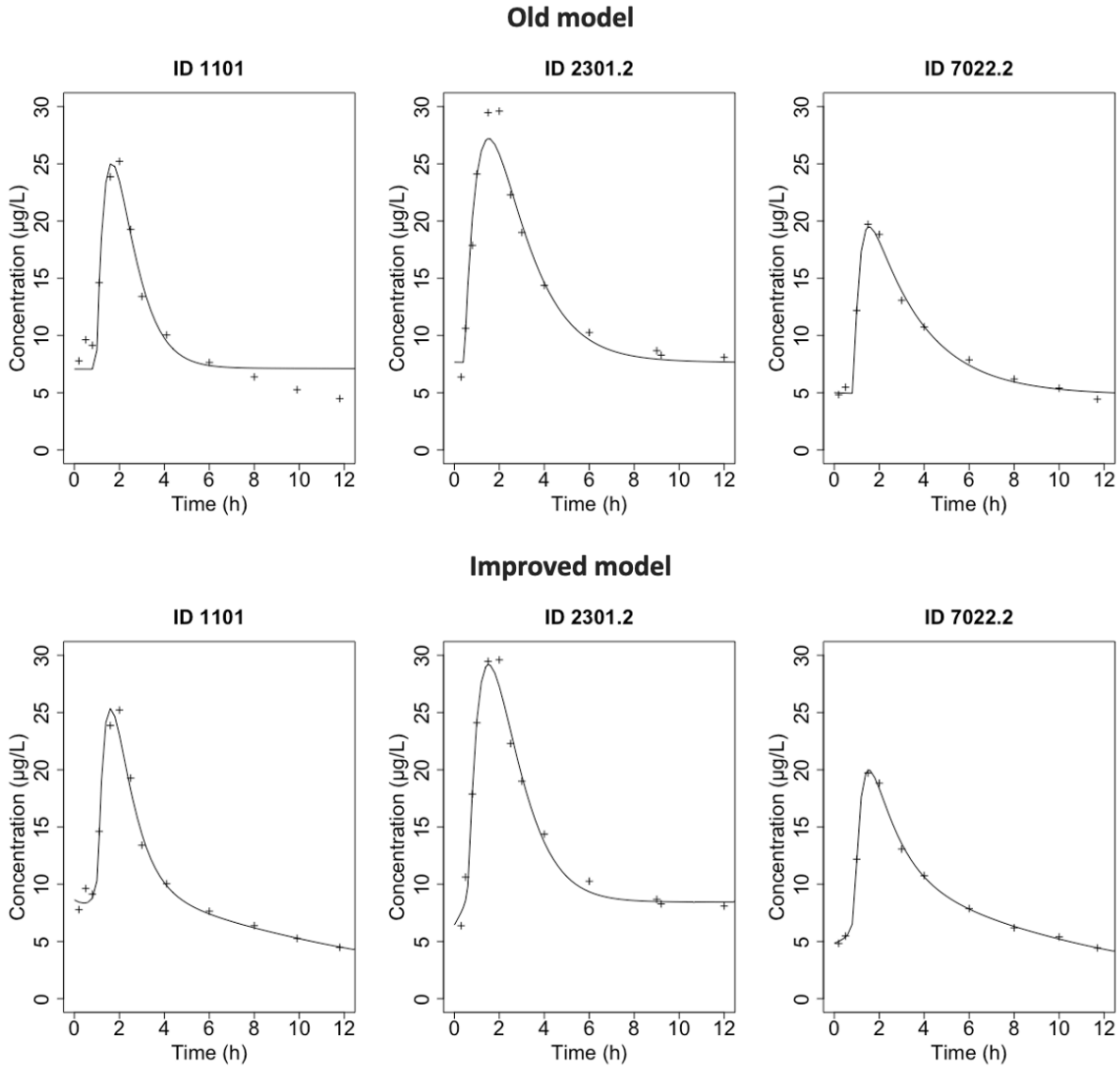

Figure 11. *Individual time-concentration plots for three individuals for Prograf® predicted by the Old model (upper row) and the Improved model (lower row).*

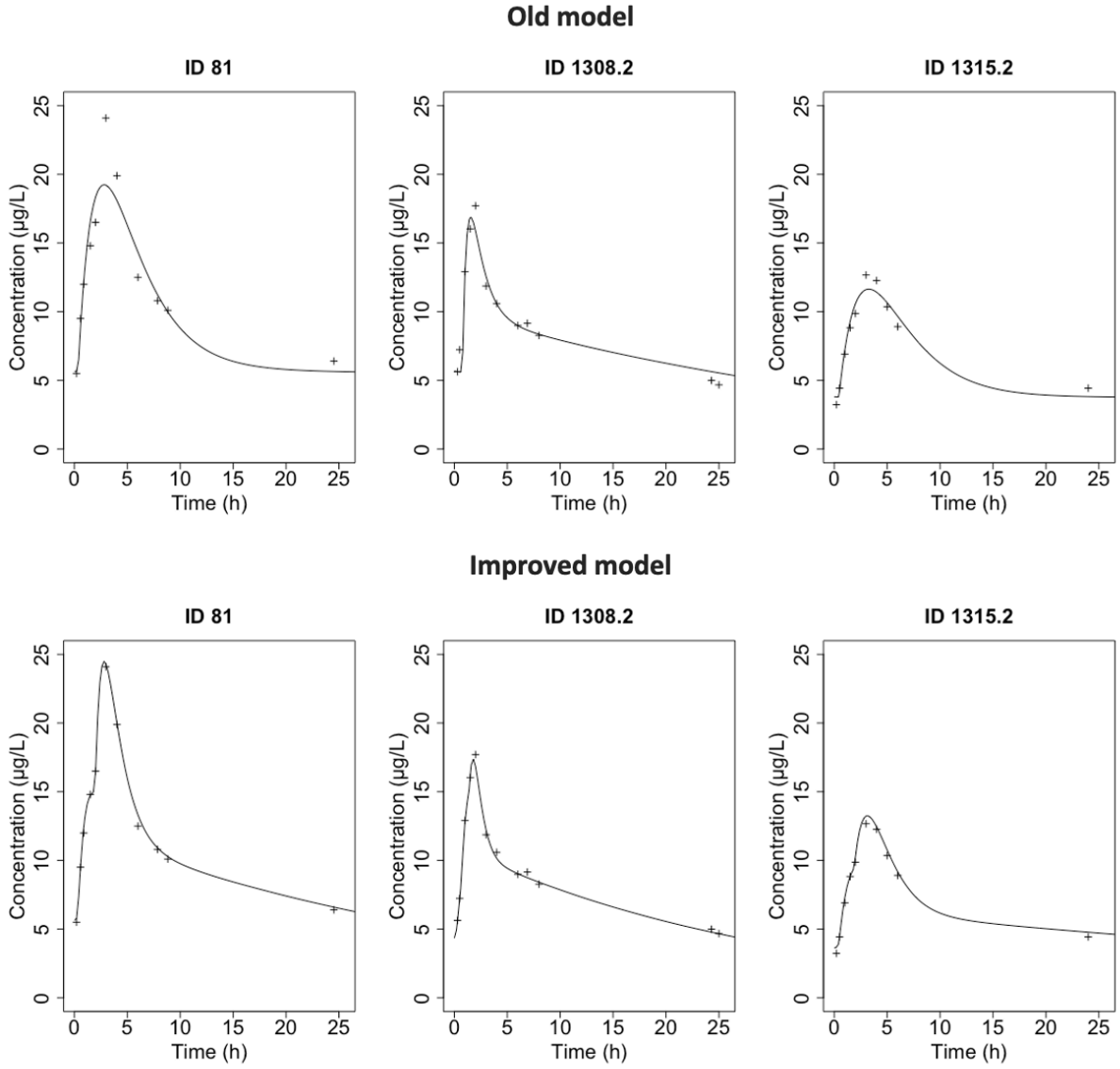

Figure 12. *Individual time-concentration plots for three individuals for Advagraf® predicted by the Old model (upper row) and the Improved model (lower row).*

3.3 External validation of the Improved model

The Improved model was run on the Validation dataset without cycling. %RMSE was 16.10 and R^2 was 0.96. Figure 13 shows population and individual OP-plots for external validation of the Improved model. %RMSE is increased from the final Improved model, and individual value of R^2 are decreased. Population value of R^2 is the same as for the final Improved model.

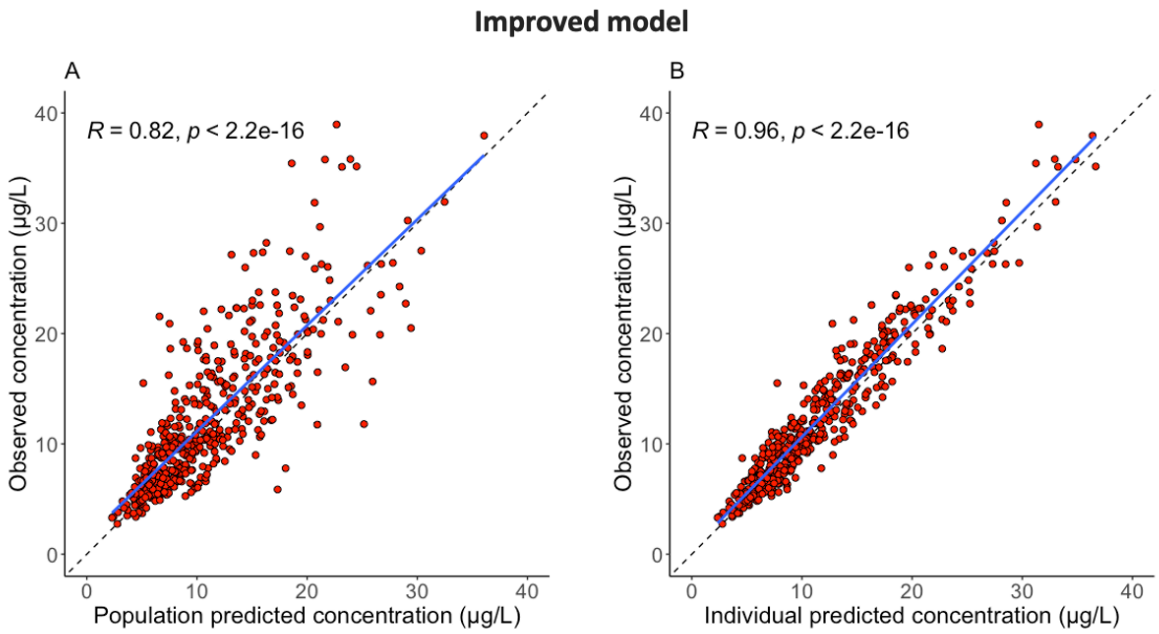

Figure 13. *Population (A) and individual (B) observed versus predicted plots of the external validation of the Improved model. R, coefficient of determination; p, probability.*

The best sampling times for tacrolimus on the Old model when using LSS have shown to be at 0, 1 and 3 hours after dosing for Prograf®, and were also used for Advagraf® with this model. LSS on the Old model gave a %RMSE for AUC of 13.1. The Old model run on the Development dataset resulted in a %RMSE for AUC of 12.4. Sampling times 0, 1 and 3 hours after dosing on the New model gave a %RMSE for AUC of 51.1. For the Improved model these sampling times resulted in a %RMSE for AUC of 11.5. The results are presented in Table 12.

Table 12. *Results from runs with limited sampling strategy on the Old model, Old model on new data, New model and Improved model. The sample times were 0, 1 and 3 hours after dosing for both Prograf® and Advagraf®.*

	Sample times	%RMSE AUC
Old model	0, 1, 3	13.1
Old model, new data	0, 1, 3	12.4
New model	0, 1, 3	51.1
Improved model	0, 1, 3	10.2

Sample times are in hours after dosing. %RMSE, percent root mean squared error of prediction; AUC, area under the plasma drug concentration–time curve.

3.3.1 LSS sampling times for the Improved model

The final Improved model was tested with different sampling times for LSS to find the optimal sampling times for both Prograf® and Advagraf® with the Improved model. An extract of the times tested, and the result of %RMSE of AUC are presented in Table 13. %RMSE of AUC was lowest at sampling times 0, 3 and 5 hours after dosing for Prograf® and 0, 2 and 6 hours after dosing for Advagraf®.

Table 13. *Results from runs using limited sampling strategy at different sampling times on the Improved model.*

Sample times Prograf®	Sample times Advagraf®	%RMSE AUC
0, 1, 3	0, 1, 3	10.2
0, 2, 4	0, 2, 4	11.5
0, 3, 5	0, 3, 5	8.1
0, 2, 6	0, 2, 6	10.2
0, 3, 5	0, 2, 6	5.0

Sample times are in hours after dosing. %RMSE, percent root mean squared error of prediction; AUC, area under the plasma drug concentration–time curve.

Table 14 shows the best sampling times of the Improved model and sampling times 0, 1, 3 hours after dosing compared to the best sampling times of the Old model and the New model. %RMSE of AUC for the Improved model is greatly reduced from the New model, and from the Old model.

Table 14. *Results from runs with limited sampling strategy on the Old model, New model and Improved model.*

	Sample times Prograf®	Sample times Advagraf®	%RMSE AUC
Old model	0, 1, 3	0, 1, 3	13.1
New model	0, 1, 3	0, 1, 3	51.1
Improved model	0, 1, 3	0, 1, 3	10.2
Improved model	0, 3, 5	0, 2, 6	5.0

Sample times are in hours after dosing. %RMSE, percent root mean squared error of prediction; AUC, area under the plasma drug concentration–time curve.

Figure 14 shows individual time-concentration plots for three individuals from LSS of Prograf® from the Old model using sampling times 0, 1 and 3 hours after dosing (middle row) and the Improved model using sampling times 0, 3 and 5 hours after dosing (lower row),

compared to observed concentrations (upper row). Both models show underestimation of higher concentrations for Prograf®. The Improved model provides slightly better prediction of the concentrations at the later times of the dosing interval.

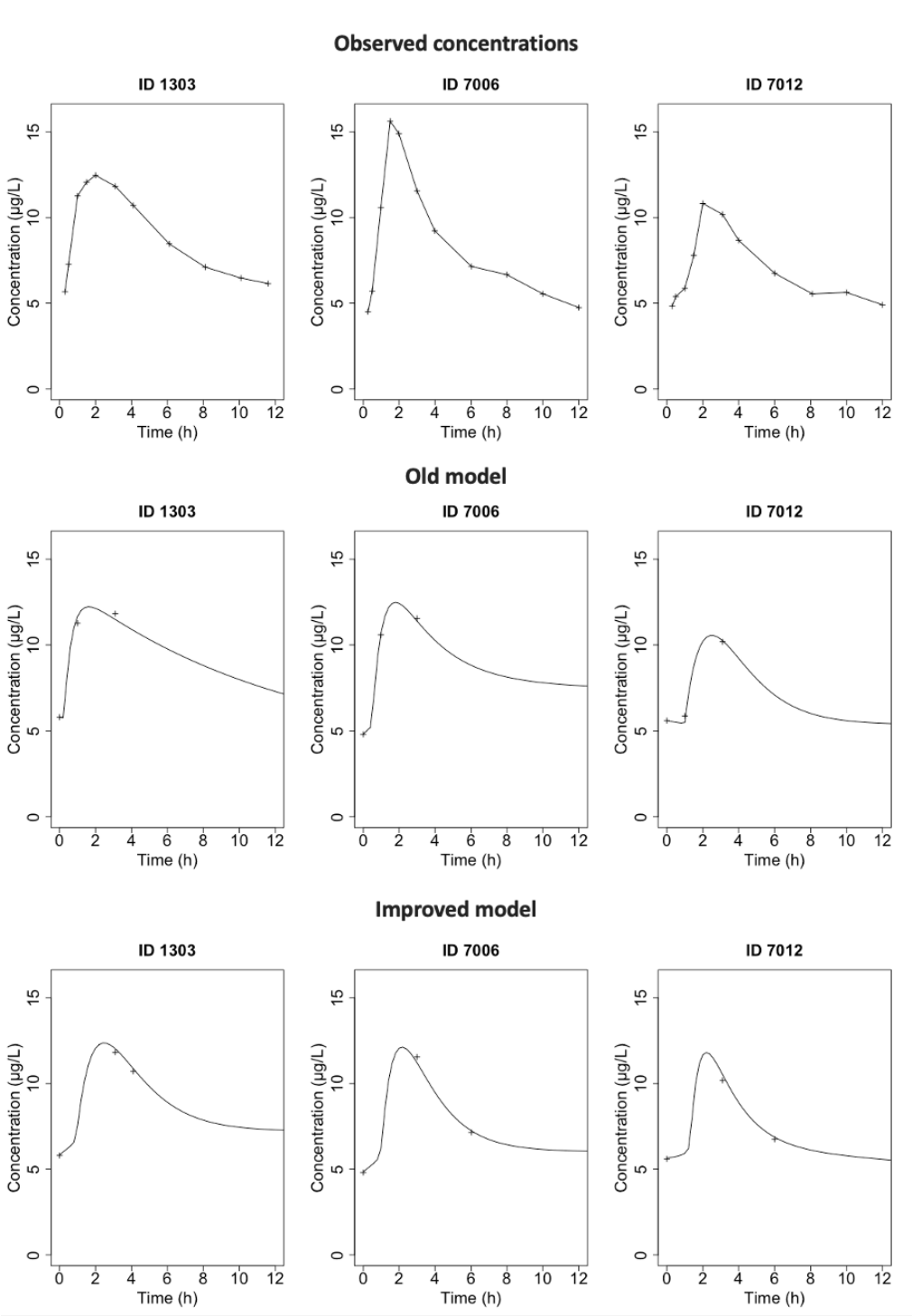

Figure 14. *Individual time-concentration plots for three individuals for Prograf® predicted by the Old model using sampling times 0, 1 and 3 hours after dosing (middle row) and the Improved model using sampling times 0, 3 and 5 hours after dosing (lower row), compared to observed concentrations (upper row).*

Figure 15 shows individual time-concentration plots for three individuals from LSS of Advagraf® from the Old model using sampling times 0, 1 and 3 hours after dosing (middle row) and the Improved model using sampling times 0, 2 and 6 hours after dosing (lower row), compared to observed concentrations (upper row). The plots show that both the Improved model and the Old model over- and underestimates the concentrations for Advagraf®. The Improved model overestimates the C_{max} more often than the Old model, and the Old model more often underestimates the concentrations at the later times of the dosing interval.

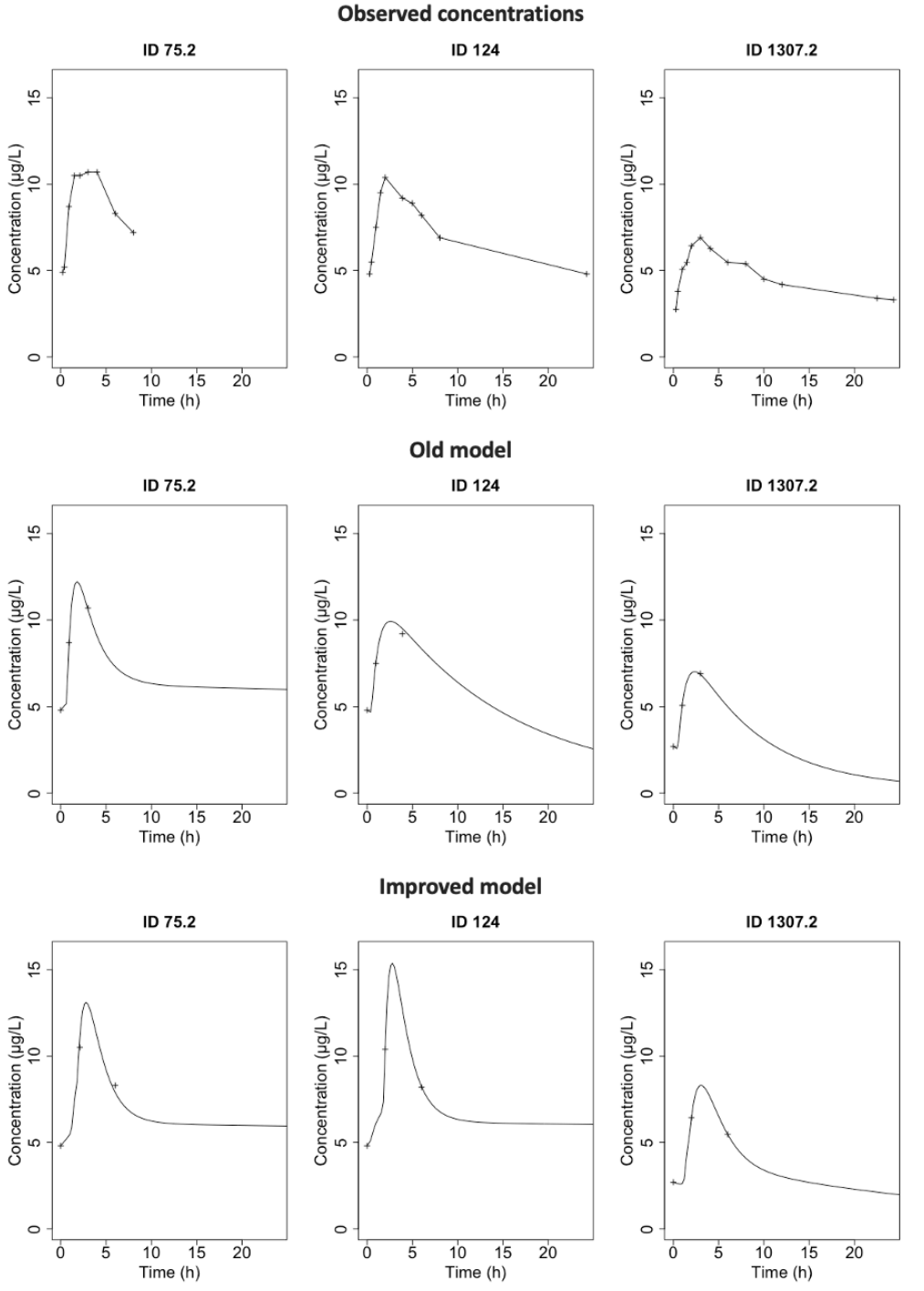

Figure 15. *Individual time-concentration plots for three individuals for Advagraf® predicted by the Old model using sampling times 0, 1 and 3 hours after dosing (middle row) and the Improved model using sampling times 0, 2 and 6 hours after dosing (lower row), compared to observed concentrations (upper row).*

3.4 Extrapolation of the Improved model to the paediatric population

The Improved model was run on the datasets from the paediatric population without cycling. In addition, the Old model was run on the same datasets without cycling for comparison. The results are presented in Table 15. %RMSE was lower for the Old model than the Improved model on both datasets. For both models %RMSE was lower for the Rich paediatric dataset than the Paediatric dataset.

Table 15. *Result from the extrapolation of the Old model and the Improved model to the paediatric population. The Paediatric dataset included all observations from time 0 to 48 hours. The Rich paediatric dataset contained only data with at least two tacrolimus measurements per dose interval.*

	Old model	**Improved model**
Paediatric dataset		
%RMSE	31.1	44.8
R^2	0.79	0.66
Rich paediatric dataset		
%RMSE	27.7	37.5
R^2	0.83	0.76

%RMSE, percent root mean squared error of prediction; R^2, coefficient of determination.

Figure 16 shows individual OP plots for the Old model (upper row) and the Improved model (lower row) run on the Paediatric dataset and the Rich paediatric dataset. R^2 was higher for the Old model than the Improved model on both datasets, and higher for the Rich paediatric dataset than for the Paediatric dataset.

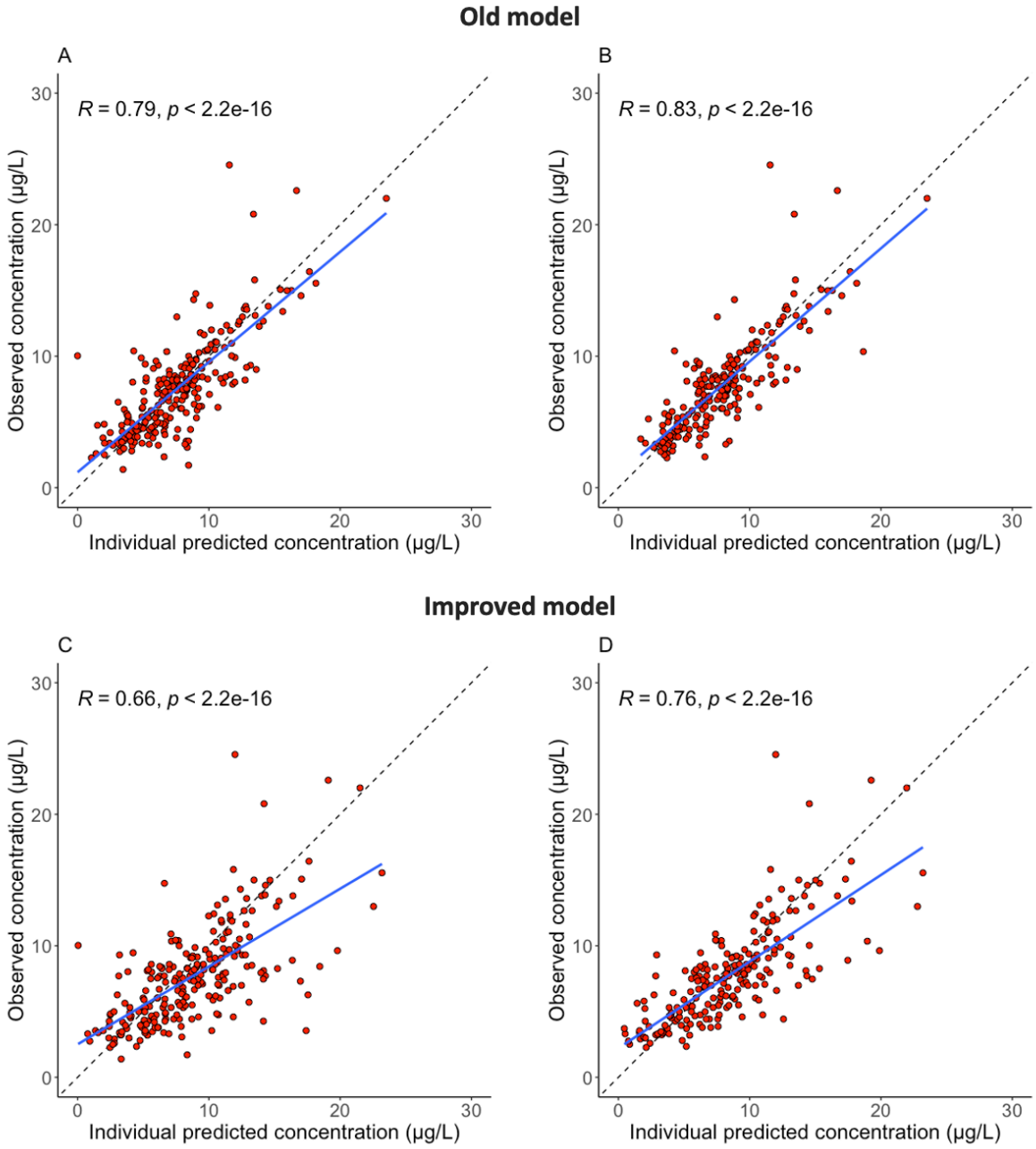

Figure 16. *Individual observed versus predicted plots for the Old model on the Paediatric dataset (A) and the Rich paediatric dataset (B), and for the Improved model on the Paediatric dataset (C) and the Rich paediatric dataset (D). R, coefficient of determination; p, probability.*

Figure 17 shows plots of mean individual prediction error against age and the RMSE against age for the Improved model on the Rich paediatric dataset. The plots show that there is no pattern in the prediction error or RMSE against age, and there is no indication that the error decreases with higher age.

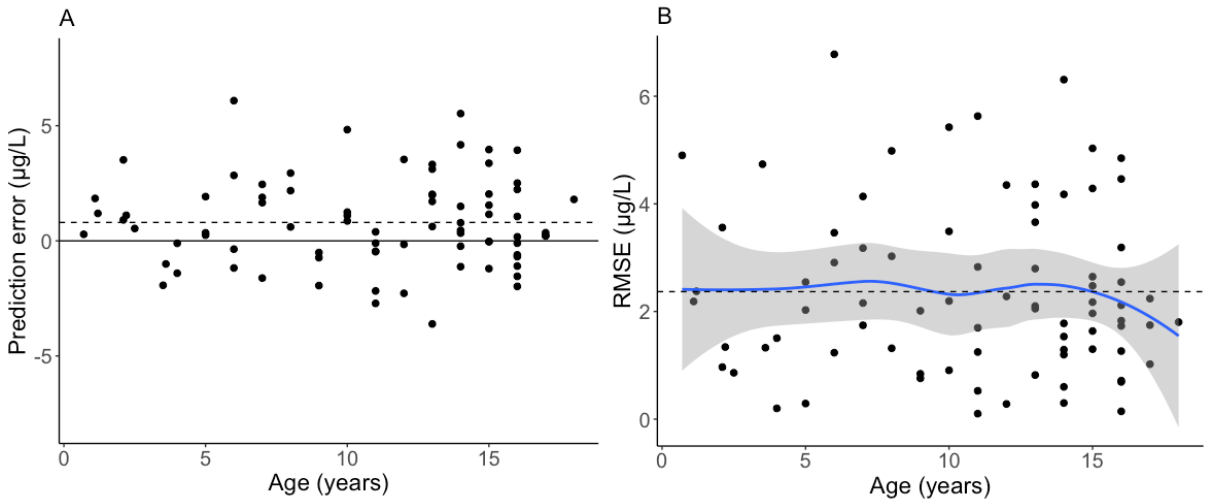

Figure 17. *Plots of mean individual prediction error (µg/L) against age (A) and the RMSE (µg/L) against age (B) for the Improved model on the Rich paediatric dataset. The dotted line in both plots shows the average error. RMSE, root mean squared error of prediction.*

The result from the Improved model run on the Rich paediatric dataset without allometric scaling to BSA is presented in Table 16 compared to the run with allometric scaling. For the Improved model run on the Rich paediatric dataset without allometric scaling %RMSE was 35.1 and R^2 was 0.74. Both %RMSE and R^2 are slightly decreased from the run on the dataset with allometric scaling. Figure 18 shows individual OP plots for the Improved model with and without allometric scaling to BSA.

Table 16. *Result from the extrapolation of the Improved model to the Rich paediatric dataset with and without allometric scaling to body surface area.*

	Allometric scaling to BSA	**No allometric scaling to BSA**
%RMSE	37.5	35.1
R^2	0.76	0.74

BSA, body surface area; %RMSE, percent root mean squared error of prediction; R^2, coefficient of determination.

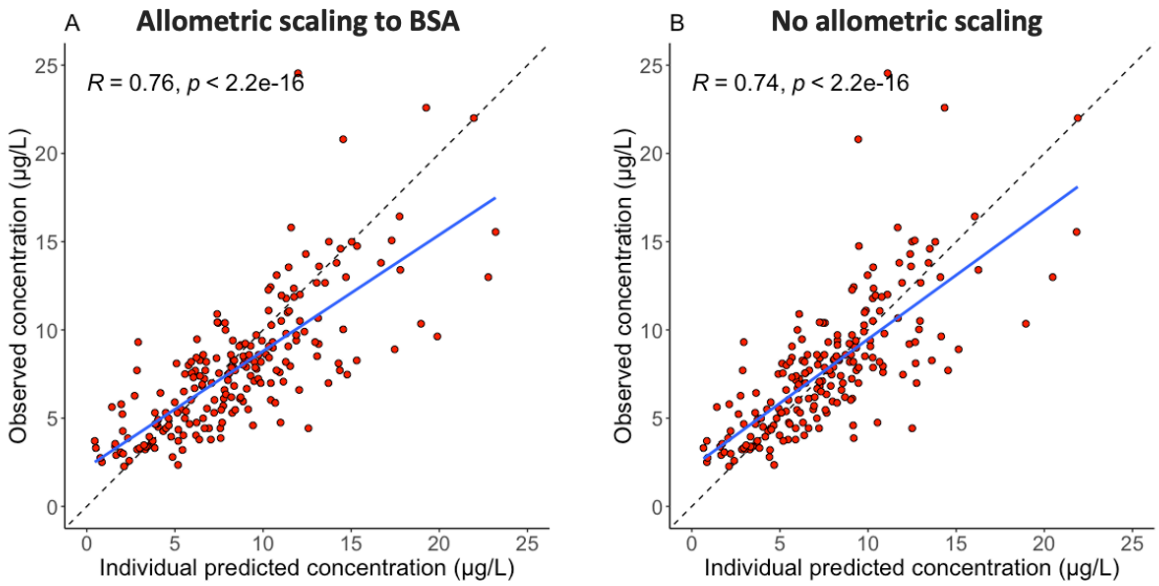

Figure 18. *Individual observed versus predicted plots for the Improved model with allometric scaling to body surface area (A) and without allometric scaling (B). BSA, body surface area; R, coefficient of determination; p, probability.*

Figure 19 shows plots of mean individual prediction error against age for the Improved model with and without allometric scaling to BSA. The plots show some, but not great improvement in the prediction for the model without allometric scaling. Where the model with allometric scaling tend to overestimate, the model without allometric scaling seems to be underestimating some more. Overall, the model without allometric scaling seems to underestimate for the lower ages and overestimate for the higher ages.

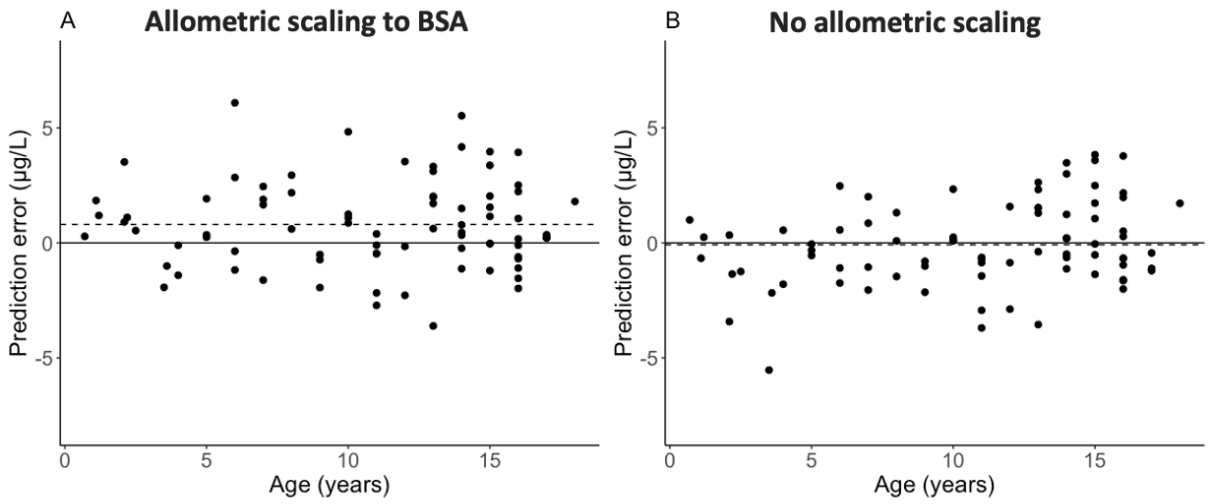

Figure 19. *Plots of mean individual prediction error against age for the Improved model with allometric scaling to body surface are (A) and without allometric scaling (B). The dotted line in both plots shows the average error. BSA, body surface area.*

4 Discussion

In this thesis a nonparametric mixed-effects tacrolimus PopPK model for adult renal transplant recipients was further developed and improved. The Improved model, a five-compartment model including the Heaviside step function with a fixed LAM, was attempted extrapolated to the paediatric population. The Improved model displayed a good predictability of tacrolimus concentrations in the adult population. However, extrapolation to the paediatric population did not display adequate prediction abilities.

4.1 Nonparametric modelling approach

A nonparametric approach was chosen for the modelling. A parametric model has the ability to separate interpatient variability from intrapatient variability, but it assumes that the parameter distribution is the same for the whole population and often normal or lognormal (47, 52). It is not able to efficiently detect unanticipated subpopulations that may affect the PK properties of the drug as a nonparametric model does. A nonparametric model can provide an improved description of the true distribution of parameters, detect unexpected subpopulations (47, 54) and are relevant for designing precise individual dosage regimens (53). For these reasons, a nonparametric approach was chosen.

4.2 Model development

4.2.1 Inclusion of the Heaviside step function and fixed LAM

The Old model with lag time had a good prediction of C0. However, the time-concentration plots show that the model's prediction of the C_{max} is suboptimal as it often tends to be underestimated. As a result, the model's prediction of AUC might be improved. The model's description of the absorption phase was identified as a possible point of improvement.

The Heaviside step function was included instead of lag time in the New model to describe the absorption phase. Lag time is commonly used in PopPK modelling for describing the delay in absorption of tacrolimus. Whereas lag time provides a lag phase followed by a constant rate of absorption, the Heaviside step function can capture more complex absorption patterns. The Heaviside step function can be modified and optimized to fit individual patient

data, accounting for inter-individual variability in drug absorption, and provide a gradual transition between the compartments. Advagraf exhibits a complex absorption profile that is characterized by an initial lag phase followed by a rapid increase in plasma concentration, and then a gradual decrease over time. The traditional lag time model cannot fully capture this behaviour, as it assumes a constant rate of absorption following the lag phase. The Heaviside step function in combination with transit compartments provides a more physiological representation of drug absorption by allowing for a gradual absorption and transition between the compartments.

LAM was included in the Heaviside step function to control the amount of smoothing in the model. In the New model LAM was not set as a fixed value which allowed for the model to search for a value of LAM for each individual. This led to an over-parameterized model. As a result, the model performed poorly on LSS data.

During model improvement values of LAM from 2 to 30 were tested. As a large value of LAM will provide a steep curve that resembles the use of the standard lag time, no values higher than 30 were tested. The models with the lower values of LAM performed poorly on the internal validation. External validation and runs with LSS of the models with different fixed values of LAM showed inconsistent results. There was no clear pattern in the results with increasing value of LAM, and the values of LAM that performed best on external validation did not necessarily do best with LSS.

In the final Improved model LAM was set to “22!”. This means that instead of estimating an individual value of LAM for each patient, the model sets the value of LAM to 22 for all patients. Setting the value of LAM to “22” without an exclamation point (!), which makes the model estimate the value of LAM starting at 22, was also tested, but resulted in the computer not being able to run the model.

The time-concentration plots for the Improved model shows how it better predicts the C_{max} for both formulations compared to the Old model on the Development dataset. The inclusion of additional lag compartments for Advagraf® in the model resulted in a more jagged curve that closely follows the data. For LSS the Improved model provided a slightly better prediction of the later times of the dosing interval for Prograf®. For LSS of Advagraf® the Improved model tended to overestimate the C_{max} whereas the Old model underestimated the concentrations at the later times of the dosing interval.

4.3 External validation

Due to lack of an independent validation cohort, the adult population dataset was randomly split in two to create the datasets for model development and validation. Although the dataset used for external validation did not include the same patients as the dataset used for development it does not provide a complete external validation as the data is derived from the same sampling as the dataset used for training the model.

4.4 Extrapolation of the Improved model to the paediatric population

Previous extrapolation of the Intermediate model to paediatric renal transplant recipients showed promising results (88). However, extrapolation of the Improved model to the paediatric population displayed poor prediction abilities. The paediatric population have a greater proportion of intrapatient variability compared to the adult population, in addition to a higher V_d and CL (32-34), and therefore this was somewhat expected. However, the promising results of the extrapolation of the Intermediate model (88) and the inclusion of rich data in the Improved model which allowed for a better description of the PK properties of the drug, raised hope for a more successful extrapolation.

The poor results of the extrapolation can be due to that the model was trained on an adult population with different PK properties of tacrolimus than the paediatric population. In addition, the paediatric population was more heterogeneous than the adult population which may also have impacted the model's accuracy. One could argue that because of these differences a model for the paediatric population should be developed on data from the population for which it is intended to be used. However, due to limited available rich paediatric data it would be difficult to develop a model with detailed description of the PK properties. The lack of rich paediatric data may also be a reason for the poor results of the extrapolation. The Rich paediatric dataset contained only data with at least two tacrolimus measurements per dose interval. Some of the paediatric patients had only one measurement per dose interval and were therefor excluded from the dataset. Due to this, the Rich paediatric dataset included less data. In addition, although the dataset was named Rich paediatric dataset, the average number of tacrolimus samples per patient was 2, meaning it for most of the patients did not actually contain rich data, defined as 6-8 samples per dose interval.

Overall, the extrapolation of the Improved model did not provide adequate predictions, and there was no indication that the performance of the model in the youngest patients was worse than in the older patients in the paediatric population. Consequently, it was not possible to determine the lower limit of age for when the adult model is still valid.

4.4.1 Effect of allometric scaling to body size

It is common for the paediatric population to have a much wider relative range in body size than adults in PK studies, and so allometric scaling to BSA was added to the model to adjust for the differences in body size between the populations. Allometric scaling can prevent PK parameters that normally are functions of body size, such as CL and V_d, and other important covariates from being masked by the effect of body size (36, 100). Earlier developed paediatric tacrolimus PopPK models for renal transplant recipients (62, 72-74, 81, 82), liver transplant recipients (60, 61, 65, 67, 71, 76, 79, 80, 101, 102), hematopoietic stem cell transplant recipients (64, 66, 77, 103, 104) and patients with lupus nephritis (105) often includes body size scaling.

However, as mentioned earlier the relationship of CL and weight for tacrolimus in children is not linear (24, 32) and as allometric scaling to body size assumes that CL is proportional to body size this might not be an optimal solution for tacrolimus. Successful paediatric PopPK models for tacrolimus without the inclusion of body size have been developed (63, 78, 106, 107). Also, previous testing of tacrolimus PopPK models at the renal transplant centre at the Oslo University Hospital, Rikshospitalet indicated that a model not allometrically scaled to body size may be superior in the paediatric population compared to a model adjusted to body size. However, the results in this master's thesis from the extrapolation of the Improved model without allometric scaling to BSA did not display an outstanding improvement of the results compared to the extrapolation with allometric scaling.

4.5 Future perspectives

The inclusion of fixed LAM in the Heaviside step function improved the model's performance on LSS. However, the individual time-concentration plots show that the model tends to both over- and underestimate. There are no available publications on the implementation of the Heaviside step function to describe the absorption of tacrolimus.

Before the model can be used in the clinic further investigation of the effect of the Heaviside step function and different values of LAM is needed.

The testing of the optimal sampling times for LSS for the Improved model found different sampling times for Prograf® and Advagraf®. The Old model, currently in use at the clinic, uses the optimal sampling times found for Prograf® for both formulations. The findings in this master's thesis might suggest that further testing of the optimal sampling times for Advagraf® might improve the model's performance with a LSS.

The Improved model did not provide reliable predictions for the paediatric population. The model needs further testing and improvement before being implemented in the clinic. In addition, further improvement and testing of the model is necessary before establishing the effect of allometric scaling on the paediatric population. Although the findings of this thesis might indicate an improvement of the model when not including allometric scaling. Future testing of extrapolation to the paediatric population should ideally involve rich paediatric data. This could possibly improve the performance of the model substantially.

5 Conclusion

In this thesis, the improvement of a PopPK model for tacrolimus resulted in a model with better performance when applied to a LSS for estimating AUC. The Improved model was not successfully extrapolated to the paediatric population. There was no indication that the performance of the model in the youngest patients was worse than in the older patients in the paediatric population. Consequently, it was not possible to determine the lower limit of age for when the adult model is still valid. Further improvement of the model is necessary before it can be implemented in the clinic for paediatric patients. The extrapolation of the model without using allometric scaling to body size showed some improvement of the model and might indicate that a model without allometric scaling could be more beneficial in the paediatric population. Before the effect of allometric scaling can be fully established, further testing of an improved model is needed.

Bibliography

1. Merrill JP, Murray JE, Harrison JH, Guild WR. Successful homotransplantation of the human kidney between identical twins. J Am Med Assoc. 1956;160(4):277-82.

2. McCauley J. A History of Kidney Transplantation. In: Ramirez CGB, McCauley J, editors. Contemporary Kidney Transplantation: Springer Cham; 2018. p. 1-23.

3. Thorsby E. Norsk transplantasjonsmedisin gjennom 50 år. Tidsskrift for Den norske legeforening. 2006;126(24):3305-10.

4. Heldal K. Nyretransplantasjon før og nå. Tidsskrift for Den norske legeforening. 2021;126.

5. Halloran PF. Immunosuppressive drugs for kidney transplantation. The New England journal of medicine. 2004;351(26):2715–29.

6. Reisæter AV, Åsberg A, Midtvedt K. Dagens og fremtidens immunsuppresjon etter nyretransplantasjon. Indremedisineren. 2019.

7. Hagness M, Midtvedt K, Reisæter AV, Skauby M. Protokoll nyretransplantasjon Norsk Nyremedisinsk forening. 2021 [cited 2022 Oct 6]. Available from: https://www.nephro.no/veileder/protokoll2021/2021Nyretxprotokoll.pdf.

8. Norsk legemiddelhåndbok. Kalsinevrinhemmere. 2017 [cited 2022 Nov 23]. Available from: https://www.legemiddelhandboka.no/L18.2/Kalsinevrinhemmere.

9. Allison AC. Mechanisms of action of mycophenolate mofetil. Lupus. 2005;14(1_suppl):2–8.

10. Norsk legemiddelhåndbok. Mykofenolat 2018 [cited 2022 Nov 23]. Available from: https://www.legemiddelhandboka.no/L18.1.2/Mykofenolat.

11. Dashti-Khavidaki S, Saidi R, Lu H. Current status of glucocorticoid usage in solid organ transplantation. World journal of transplantation. 2021;11(11):443-65.

12. Naesens M, Kuypers DR, Sarwal M. Calcineurin inhibitor nephrotoxicity. Clin J Am Soc Nephrol. 2009;4(2):481-508.

13. Schreiber SL, Crabtree GR. The mechanism of action of cyclosporin A and FK506. Immunol Today. 1992;13(4):136-42.

14. European Medicines Agency. Advagraf : EPAR - Product Information. 2009 [cited 2023 Jan 17].

15. Brooks E, Tett SE, Isbel NM, Staatz CE. Population Pharmacokinetic Modelling and Bayesian Estimation of Tacrolimus Exposure: Is this Clinically Useful for Dosage Prediction Yet? Clin Pharmacokinet. 2016;55(11):1295-335.

16. Yu M, Liu M, Zhang W, Ming Y. Pharmacokinetics, Pharmacodynamics and Pharmacogenetics of Tacrolimus in Kidney Transplantation. Curr Drug Metab. 2018;19(6):513-22.

17. Green MD, Michaels MG. Tacrolimus: effects and side effects. Pediatr Infect Dis J. 1999;18(4):372-3.

18. Staatz CE, Tett SE. Clinical pharmacokinetics and pharmacodynamics of tacrolimus in solid organ transplantation. Clin Pharmacokinet. 2004;43(10):623-53.

19. Venkataramanan R, Swaminathan A, Prasad T, Jain A, Zuckerman S, Warty V, et al. Clinical pharmacokinetics of tacrolimus. Clin Pharmacokinet. 1995;29(6):404-30.

20. Tuteja S, Alloway RR, Johnson JA, Gaber AO. The effect of gut metabolism on tacrolimus bioavailability in renaltransplant recipients. Transplantation. 2001;71(9):1303-7.

21. Dai Y, Hebert MF, Isoherranen N, Davis CL, Marsh C, Shen DD, et al. EFFECT OF CYP3A5 POLYMORPHISM ON TACROLIMUS METABOLIC CLEARANCE IN VITRO. Drug Metab Dispos. 2006;34(5):836-47.

22. Schuetz E, Kuehl P, Zhang J, Lin Y, Lamba J, Assem M, et al. Sequence diversity in CYP3A promoters and characterization of the genetic basis of polymorphic CYP3A5 expression. Nat Genet. 2001;27(4):383-91.

23. Haufroid V, Wallemacq P, VanKerckhove V, Elens L, De Meyer M, Eddour DC, et al. CYP3A5 and ABCB1 Polymorphisms and Tacrolimus Pharmacokinetics in Renal Transplant Candidates: Guidelines from an Experimental Study. Am J Transplant. 2006;6(11):2706-13.

24. Lancia P, Jacqz-Aigrain E, Zhao W. Choosing the right dose of tacrolimus. Arch Dis Child. 2015;100(4):406-13.

25. Degraeve AL, Moudio S, Haufroid V, Chaib Eddour D, Mourad M, Bindels LB, et al. Predictors of tacrolimus pharmacokinetic variability: current evidences and future perspectives. Expert opinion on drug metabolism & toxicology. 2020;16(9):769–82.

26. Anews L, de Winter B, Tang J, Shuker N, Bouamar R, van Schaik R, et al. Overweight Kidney Transplant Recipients Are at Risk of Being Overdosed Following Standard Bodyweight-Based Tacrolimus Starting Dose. Transplant Direct. 2017;3(2):e129-e.

27. Undre NA, Schäfer A. Factors affecting the pharmacokinetics of tacrolimus in the first year after renal transplantation. Transplantation proceedings. 1998;30(4):1261–3.

28. Gelder T. Drug Interactions with Tacrolimus. Drug Safety. 2002;25(10):707–12.

29. Størset E, Holford N, Midtvedt K, Bremer S, Bergan S, Åsberg A. Importance of hematocrit for a tacrolimus target concentration strategy. Eur J Clin Pharmacol. 2014;70(1):65-77.

30. Hebert MF, Zheng S, Hays K, Shen DD, Davis CL, Umans JG, et al. Interpreting tacrolimus concentrations during pregnancy and postpartum. Transplantation. 2013;95(7):908-15.

31. Bekele F, Bereda G, Tamirat L, Geleta BA, Jabessa D. "Childrens are not just "little adults". The rate of medication related problems and its predictors among patients admitted to pediatric ward of southwestern Ethiopian hospital: A prospective observational study. Ann Med Surg (Lond). 2021;70:102827.

32. Fernandez de Gatta MdM, Santos-Buelga D, Dominguez-Gil A, Garcia MJ. Immunosuppressive Therapy for Paediatric Transplant Patients: Pharmacokinetic Considerations. Clin Pharmacokinet. 2002;41(2):115-35.

33. Jain AB, Fung JJ, Tzakis AG, Venkataramanan R, Abu-Elmagd K, Alessiani M, et al. Comparative study of cyclosporine and FK 506 dosage requirements in adult and pediatric orthotopic liver transplant patients. Transplant Proc. 1991;23(6):2763-6.

34. Wallemacq PE, Furlan V, Möller A, Schäfer A, Stadler P, Firdaous I, et al. Pharmacokinetics of tacrolimus (FK506) in paediatric liver transplant recipients. Eur J Drug Metab Pharmacokinet. 1998;23(3):367-70.

35. Sharma V, McNeill JH. To scale or not to scale: the principles of dose extrapolation. Br J Pharmacol. 2009;157(6):907-21.

36. Meibohm B, Läer S, Panetta JC, Barrett JS. Population pharmacokinetic studies in pediatrics: issues in design and analysis. The AAPS journal. 2005;7(2):E475–E487.

37. Kang JS, Lee MH. Overview of therapeutic drug monitoring. The Korean journal of internal medicine. 2009;24(1):1–10.

38. Størset E, Åsberg A, Skauby M, Neely M, Bergan S, Bremer S, et al. Improved Tacrolimus Target Concentration Achievement Using Computerized Dosing in Renal Transplant Recipients—A Prospective, Randomized Study. Transplantation. 2015;99(10):2158-66.

39. Bergan S BN. Persontilpasset behandling med biologiske legemidler. Norsk Farmaceutisk Tidsskrift. 2018;1:40-3.

40. Gustavsen MT, Midtvedt K, Vethe NT, Robertsen I, Bergan S, Åsberg A. Tacrolimus Area Under the Concentration Versus Time Curve Monitoring, Using Home-Based Volumetric Absorptive Capillary Microsampling. Ther Drug Monit. 2020;42(3):407-14.

41. Brunet M, Gelder T, Asberg A, Haufroid V, Hesselink D, Langman L, et al. Therapeutic Drug Monitoring of Tacrolimus-Personalized Therapy: Second Consensus Report. Ther Drug Monit. 2019;41(3):261-307.

42. Wallemacq P, Armstrong VW, Brunet M, Haufroid V, Holt DW, Johnston A, et al. Opportunities to optimize tacrolimus therapy in solid organ transplantation: Report of the european consensus conference. Ther Drug Monit. 2009;31(2):139-52.

43. Kershner RP, Fitzsimmons WE. Relationship of FK506 whole blood concentrations and efficacy and toxicity after liver and kidney transplantation. Transplantation. 1996;62(7):920-6.

44. Gabrielsson J, Weiner D. Non-compartmental analysis. Methods Mol Biol. 2012;929:377-89.

45. Derendorf H, Schmidt S, Rowland M. Rowland and Tozer's clinical pharmacokinetics and pharmacodynamics : concepts and applications. Fifth edition. ed. Philadelphia: Wolters Kluwer; 2020.

46. Mould DR, Upton RN. Basic concepts in population modeling, simulation, and model-based drug development-part 2: introduction to pharmacokinetic modeling methods. CPT Pharmacometrics Syst Pharmacol. 2013;2(4):e38.

47. Tatarinova T, Neely M, Bartroff J, van Guilder M, Yamada W, Bayard D, et al. Two general methods for population pharmacokinetic modeling: non-parametric adaptive grid and non-parametric Bayesian. J Pharmacokinet Pharmacodyn. 2013;40(2):189-99.

48. van der Meer AF, Marcus MAE, Touw DJ, Proost JH, Neef C. Optimal Sampling Strategy Development Methodology Using Maximum A Posteriori Bayesian Estimation. Ther Drug Monit. 2011;33(2):133-46.

49. Ette EI, Williams PJ. Population pharmacokinetics I: background, concepts, and models. Ann Pharmacother. 2004;38(10):1702-6.

50. Natvig B. En introduksjon til Bayesiansk statistikk og beslutningsteori: Matematisk institutt, Universitetet i Oslo; 1997.

51. Thoon AH, Whiting B. Bayesian parameter estimation and population pharmacokinetics. Clin Pharmacokinet. 1992;22(6):447-67.

52. Jelliffe R, Schumitzky A, Van Guilder M, Wang X, Leary R. Population Pharmacokinetic Models: Parametric and Nonparametric Approaches [cited 2022 Nov 21]. Available from: http://www.lapk.org/pubsinfo/TechReports/MathMod1.pdf.

53. Goutelle S, Woillard JB, Neely M, Yamada W, Bourguignon L. Nonparametric Methods in Population Pharmacokinetics. J Clin Pharmacol. 2022;62(2):142-57.

54. Neely MM, van Guilder MM, Yamada WW, Schumitzky AA, Jelliffe RR. Accurate detection of outliers and subpopulations with Pmetrics, a non-parametric and parametric pharmacometric modeling and simulation package for R. Ther Drug Monit. 2012;34(4):467-76.

55. The R Foundation. What is R? The R Project for Statistical Computing [cited 2022 Sep 7]. Available from: https://www.r-project.org/about.html.

56. Yamada W, Bartroff J, Bayard D, Burke J, Van Guilder M, Jelliffe R, et al. The nonparametric adaptive grid algorithm for population pharmacokinetic modeling. Technical Report, LAPK, USC, Laboratory of Applied Pharmacokinetics; 2012.

57. Yamada WM, Neely MN, Bartroff J, Bayard DS, Burke JV, Guilder MV, et al. An Algorithm for Nonparametric Estimation of a Multivariate Mixing Distribution with Applications to Population Pharmacokinetics. Pharmaceutics. 2020;13(1).

58. Jelliffe RW, Neely M. Individualized Drug Therapy for Patients: Elsevier Science; 2016.

59. Fukudo M, Yano I, Shinsako K, Katsura T, Takada Y, Uemoto S, et al. Prospective Evaluation of the Bayesian Method for Individualizing Tacrolimus Dose Early After Living-Donor Liver Transplantation. J Clin Pharmacol. 2009;49(7):789-97.

60. Riva N, Woillard JB, Distefano M, Moragas M, Dip M, Halac E, et al. Identification of Factors Affecting Tacrolimus Trough Levels in Latin American Pediatric Liver Transplant Patients. Liver Transpl. 2019;25(9):1397-407.

61. Wang D-D, Chen X, Fu M, Zheng Q-S, Xu H, Li Z-P. Model extrapolation to a real-world dataset: evaluation of tacrolimus population pharmacokinetics and drug interaction in pediatric liver transplantation patients. Xenobiotica. 2020;50(4):371-9.

62. Andrews L, Hesselink D, Gelder T, Koch B, Cornelissen EAM, Bruggemann RJM, et al. A Population Pharmacokinetic Model to Predict the Individual Starting Dose of Tacrolimus Following Pediatric Renal Transplantation. Clin Pharmacokinet. 2018;57(4):475-89.

63. Rower JE, Stockmann C, Linakis MW, Kumar SS, Liu X, Korgenski EK, et al. Predicting tacrolimus concentrations in children receiving a heart transplant using a population pharmacokinetic model. BMJ Paediatr Open. 2017;1(1):e000147.

64. Brooks JT, Keizer RJ, Long-Boyle JR, Kharbanda S, Dvorak CC, Friend BD. Population Pharmacokinetic Model Development of Tacrolimus in Pediatric and Young Adult Patients Undergoing Hematopoietic Cell Transplantation. Frontiers in pharmacology. 2021;12:750672–750672.

65. Fukudo M, Yano I, Masuda S, Goto M, Uesugi M, Katsura T, et al. Population pharmacokinetic and pharmacogenomic analysis of tacrolimus in pediatric living-donor liver transplant recipients. Clinical pharmacology and therapeutics. 2006;80(4):331–45.

66. Liu XL, Guan YP, Wang Y, Huang K, Jiang FL, Wang J, et al. Population Pharmacokinetics and Initial Dosage Optimization of Tacrolimus in Pediatric Hematopoietic Stem Cell Transplant Patients. Front Pharmacol. 2022;13:891648.

67. Jalil MHA, Hawwa AF, McKiernan PJ, Shields MD, McElnay JC. Population pharmacokinetic and pharmacogenetic analysis of tacrolimus in paediatric liver transplant patients. British journal of clinical pharmacology. 2014;77(1):130–40.

68. Lu Z, Bonate P, Keirns J. Population pharmacokinetics of immediate- and prolonged-release tacrolimus formulations in liver, kidney and heart transplant recipients. British journal of clinical pharmacology. 2019;85(8):1692–703.

69. Jacobo-Cabral CO, García-Roca P, Romero-Tejeda EM, Reyes H, Medeiros M, Castañeda-Hernández G, et al. Population pharmacokinetic analysis of tacrolimus in Mexican paediatric renal transplant patients: role of CYP3A5 genotype and formulation. British journal of clinical pharmacology. 2015;80(4):630–41.

70. Pasternak AL, Park JM, Pai MP. Predictive Capacity of Population Pharmacokinetic Models for the Tacrolimus Dose Requirements of Pediatric Solid Organ Transplant Recipients. 2023;45(1):95–101.

71. Guy-Viterbo V, Scohy A, Verbeeck RK, Reding R, Wallemacq P, Musuamba FT. Population pharmacokinetic analysis of tacrolimus in the first year after pediatric liver transplantation. Eur J Clin Pharmacol. 2013;69(8):1533-42.

72. Sy SKB, Heuberger J, Shilbayeh S, Conrado DJ, Derendorf H. A Markov Chain Model to Evaluate the Effect of CYP3A5 and ABCB1 Polymorphisms on Adverse Events Associated with Tacrolimus in Pediatric Renal Transplantation. AAPS J. 2013;15(4):1189-99.

73. Zhao W, Elie V, Roussey G, Brochard K, Niaudet P, Leroy V, et al. Population Pharmacokinetics and Pharmacogenetics of Tacrolimus in De Novo Pediatric Kidney Transplant Recipients. Clin Pharmacol Ther. 2009;86(6):609-18.

74. Zhao W, Fakhoury M, Baudouin V, Storme T, Maisin A, Deschênes G, et al. Population pharmacokinetics and pharmacogenetics of once daily prolonged-release formulation of tacrolimus in pediatric and adolescent kidney transplant recipients. Eur J Clin Pharmacol. 2013;69(2):189-95.

75. Guy-Viterbo V, Baudet H, Haufroid V, Elens L, Musuamba F, Lacaille F, et al. Influence of Age, Donor-Recipient CYP3A4/5 Genotypes, Fluconazole and Time Post-Transplantation On Tacrolimus Pharmacokinetics in Pediatric Liver Transplantation: Abstract# B1050. Transplantation. 2014;98:717.

76. Wallin JE, Bergstrand M, Wilczek H, Nydert PS, Karlsson MO, Staatz CE. Population pharmacokinetics of tacrolimus in pediatric liver transplantation: Early posttransplantation clearance. Ther Drug Monit. 2011;33(6):663-72.

77. Wallin J, Friberg L, Fasth A, Staatz C. Population pharmacokinetics of tacrolimus in paediatric haematopoietic stem cell transplant recipients: New initial dosage suggestions and a model based dosage adjustment tool. Ther Drug Monit. 2009;31(4):457.

78. Staatz CE, Taylor PJ, Lynch SV, Willis C, Charles BG, Tett SE. Population pharmacokinetics of tacrolimus in children who receive cut-down or full liver transplants. Transplantation. 2001;72(6):1056-61.

79. Sam WJ, Aw M, Quak SH, Lim SM, Charles BG, Chan SY, et al. Population pharmacokinetics of tacrolimus in Asian paediatric liver transplant patients. Br J Clin Pharmacol. 2000;50(6):531-41.

80. Kassir N, Labbé L, Delaloye JR, Mouksassi MS, Lapeyraque AL, Alvarez F, et al. Population pharmacokinetics and Bayesian estimation of tacrolimus exposure in paediatric liver transplant recipients. Br J Clin Pharmacol. 2014;77(6):1051-63.

81. Andrews LM, de Winter BCM, Cornelissen EAM, de Jong H, Hesselink DA, Schreuder MF, et al. A Population Pharmacokinetic Model Does Not Predict the Optimal Starting Dose of Tacrolimus in Pediatric Renal Transplant Recipients in a Prospective Study: Lessons Learned and Model Improvement. Clinical pharmacokinetics. 2020;59(5):591–603.

82. Prytuła AA, Cransberg K, Bouts AHM, van Schaik RHN, de Jong H, de Wildt SN, et al. The Effect of Weight and CYP3A5 Genotype on the Population Pharmacokinetics of Tacrolimus in Stable Paediatric Renal Transplant Recipients. Clin Pharmacokinet. 2016;55(9):1129-43.

83. Robertsen I, Åsberg A, Ingerø AO, Vethe NT, Bremer S, Bergan S, et al. Use of Generic Tacrolimus in Elderly Renal Transplant Recipients: Precaution Is Needed. Transplantation. 2015;99(3):528-32.

84. Robertsen I, Åsberg A, Midtvedt K, Vethe NT, Hartmann A, Størset E, et al. High-Dose Fish Oil Supplementation Increase Tacrolimus Exposure in Stable Renal Transplant Recipients. Transplantation. 2018;102 Suppl 7S-1(Supplement 7):S599-S.

85. Midtvedt K, Jenssen T, Hartmann A, Vethe NT, Bergan S, Havnes K, et al. No change in insulin sensitivity in renal transplant recipients converted from standard to once-daily prolonged release tacrolimus. Nephrol Dial Transplant. 2011;26(11):3767-72.

86. Gustavsen MT, Midtvedt K, Robertsen I, Woillard JB, Debord J, Klaasen RA, et al. Fasting Status and Circadian Variation Must be Considered When Performing AUC-based Therapeutic Drug Monitoring of Tacrolimus in Renal Transplant Recipients. Clin Transl Sci. 2020;13(6):1327-35.

87. Oslo University Hospital, Rikshospitalet. The PedTac study. Unpublished.

88. Storås ATM. Optimizing an adult tacrolimus population pharmacokinetic model for extrapolation to pediatric renal transplant recipients. [Master thesis]: University of Oslo; 2020.

89. Åsberg A, Midtvedt K, van Guilder M, Størset E, Bremer S, Bergan S, et al. Inclusion of CYP3A5 genotyping in a nonparametric population model improves dosing of tacrolimus early after transplantation. Transpl Int. 2013;26(12):1198-207.

90. Du Bois D, Du Bois EF. A formula to estimate the approximate surface area if height and weight be known. 1916. Nutrition. 1989;5(5):303-11; discussion 12-3.

91. Størset E, von Düring ME, Godang K, Bergan S, Midtvedt K, Åsberg A. Prediction of Fat-Free Mass in Kidney Transplant Recipients. Ther Drug Monit. 2016;38(4):439-46.

92. Legua MP, Morales I, Sánchez Ruiz LM. The Heaviside Step Function and MATLAB. In: Computational Science and Its Applications – ICCSA 2008. Berlin, Heidelberg: Springer Berlin Heidelberg; p. 1212–21.

93. Mould DR, Upton RN. Basic Concepts in Population Modeling, Simulation, and Model-Based Drug Development—Part 2: Introduction to Pharmacokinetic Modeling Methods. CPT Pharmacometrics Syst Pharmacol. 2013;2(4):1-14.

94. Bonate PL. Pharmacokinetic–Pharmacodynamic Modeling and Simulation. United States: United States: Springer; 2011.

95. Dansirikul C, Staatz CE, Duffull SB, Taylor PJ, Lynch SV, Tett SE. Sampling times for monitoring tacrolimus in stable adult liver transplant recipients. Therapeutic drug monitoring. 2004;26(6):593–9.

96. Aouam K, Chadli Z, Hammouda M, Fredj NB, Aloui S, May ME, et al. Development of Limited Sampling Strategies for the Estimation of Tacrolimus Area Under the Curve in Adult Kidney Transplant Recipients According to the Posttransplantation Time. Therapeutic drug monitoring. 2015;37(4):524–30.

97. El-Nahhas T, Popoola J, MacPhee I, Johnston A. Limited sampling strategies for estimation of tacrolimus exposure in kidney transplant recipients receiving extended-release tacrolimus preparation. Clin Transl Sci. 2022;15(1):70-8.

98. Balbontin FG, Kiberd B, Squires J, Singh D, Fraser A, Belitsky P, et al. Tacrolimus monitoring by simplified sparse sampling under the concentration time curve. Transplantation proceedings. 2003;35(7):2445–8.

99. Aumente Rubio MD, Arizón del Prado JM, López Malo de Molina MD, Cárdenas Aranzana M, Segura Saint-Gerons J, López Granados A, et al. Clinical pharmacokinetics of tacrolimus in heart transplantation: new strategies of monitoring. Transplant Proc. 2003;35(5):1988-91.

100. Germovsek E, Barker CIS, Sharland M, Standing JF. Pharmacokinetic-Pharmacodynamic Modeling in Pediatric Drug Development, and the Importance of Standardized Scaling of Clearance. Clinical pharmacokinetics. 2019;58(1):39–52.

101. Guy-Viterbo V, Baudet H, Elens L, Haufroid V, Lacaille F, Girard M, et al. Influence of donor-recipient CYP3A4/5 genotypes, age and fluconazole on tacrolimus pharmacokinetics in pediatric liver transplantation: a population approach. Pharmacogenomics. 2014;15(9):1207–21.

102. Musuamba FT, Guy-Viterbo V, Reding R, Verbeeck RK, Wallemacq P. Population pharmacokinetic analysis of tacrolimus early after pediatric liver transplantation. Therapeutic drug monitoring. 2014;36(1):54–61.

103. Wang D, Chen X, Xu H, Li Z. Population pharmacokinetics and dosing regimen optimization of tacrolimus in Chinese pediatric hematopoietic stem cell transplantation patients. Xenobiotica. 2020;50(2):188–95.

104. Zhou S, Zhang R, Lv C, Lu J, Wei Y, Li C, et al. Initial Dosage Optimization of Tacrolimus in Pediatric Patients With Thalassemia Major Undergoing Hematopoietic Stem Cell Transplantation Based on Population Pharmacokinetics. The Annals of pharmacotherapy. 2021;55(4):440–51.

105. Chen X, Wang D-D, Xu H, Li Z-P. Population pharmacokinetics model and initial dose optimization of tacrolimus in children and adolescents with lupus nephritis based on real-world data. Experimental and therapeutic medicine. 2020;20(2):1423–30.

106. Staatz CE, Tett SE. Comparison of two population pharmacokinetic programs, NONMEM and P-PHARM, for tacrolimus. European journal of clinical pharmacology. 2002;58(9):597–605.

107. Yang J-w, Liao S-s, Zhu L-q, Zhao Y, Zhang Y, Sun X-y, et al. Population pharmacokinetic analysis of tacrolimus early after Chinese pediatric liver transplantation. International journal of clinical pharmacology and therapeutics. 2015;53(1):75–83.

Appendixes

Appendix A: Model file for the Old model

```
#PRI
Ka, 0.2, 3.5
V0, 5, 500
CL0, 1, 45
Q0, 1, 140
Vp0, 300, 30000
Tlag1, 0, 2.1
Tlag2, 0, 2.1
Tlag3, 0, 2.1
A2, 0, 180000
FA0, 0.3, 1

#COV
WT
TXT
HCT
SSCONC
SEX
HGT

#SEC
BMI = WT/(HGT/100)**2
FFMf = (WT*9270)/(8780+(244*BMI))
FFM = (WT*9270)/(6680+(216*BMI))
&IF (SEX.GT.0) FFM=FFMf
FFMc = FFM/59
BMIc = BMI/26
HCTc = 0.36/HCT
CL = CL0 *HCTc*FFMc**0.75
Q = Q0*HCTc*FFMc**0.75
VP = Vp0*HCTc*FFMc
V = V0*HCTc*BMIc
KE = CL/V
KCP = Q/V
KPC = Q/VP

#INI
X(2)=SSCONC*V
X(3)=A2
IF (SSCONC.EQ.0.D0) X(3)=0

#F
FA(1)=FA0

#LAG
TLAG(1)=Tlag2*FFMc
IF (TXT.LT.8) TLAG(1)=Tlag1*FFMc
IF (TXT.GT.28) TLAG(1)=Tlag3*FFMc

#OUT
Y(1)=X(2)/V

#ERR
L=1
0.085863760,0.019489074,0.001893754,0
```

PRI, primary variables; Ka, estimated absorptions rate constant; V0, estimated volume of distribution; CL0, estimated value of clearance; Q0, estimated intercompartmental clearance; Vp0, estimated peripheral volume of distribution; Tlag1, Tlag2, Tlag3; estimated absorption lag times for three different periods of time after transplantation; A2, drug present in compartment before administered dose; FA0; estimated value of bioavailability; COV, covariates; WT, weight in kg; TXT, time after transplantation in days; HCT, haematocrit; SSCONC, steady-state concentration; HGT, height in cm; SEC, secondary variables; BMI, body mass index; FFMf, fat-free mass in kg for females; FFM, fat-free mass in kg for males; FFMc, fat-free mass formula; BMIc, body mass index formula; HCTc, haematocrit formula; CL, clearance; Q, intercompartmental clearance; VP, peripheral volume of distribution; V, volume of distribution; KE, elimination rate constant; KCP, transport rate constant from central compartment to peripheral compartment; KPC, transport rate constant from peripheral compartment back to central compartment; INI, initial conditions; X(2), X(3), amount in compartments 2 and 3 at time 0; F, bioavailability; FA(1), bioavailability formula; LAG, lag time; TLAG, absorption lag time; OUT, outputs; ERR, error; L, lambda.

Appendix B: Model file for the Intermediate model

```
#PRI
Ka1, 0.2, 3.5
Ka2, 0.2, 3.5
CL0, 4, 60
CL1, 4, 100
CL2, 4, 80
Q0, 10, 200
V0, 10, 500
Vp0, 80, 3500
Tlag1, 0, 2
Tlag2, 0, 2
Tlag3, 0, 2
TlagAdva, 0.1, 2
F1, 0.001, 1
F2, 0.001, 1
F3, 0.001, 1
Fadva, 0.1, 5
CypF, 0.01, 1
CypCl, 0.001, 3.5


#COV
STU
STER
M0F1
WTKG
HT
FFMES
TXT
HCT
AGE
CYP
ASY
RICH
EXACT
FORM
BMI
BSA


#SEC
CL = CL0 * ((BSA/1.98)**0.75)* 39.7
&IF(TXT<14) CL =CL1 * ((BSA/1.98)**0.75)* 39.7
&IF(TXT>42) CL =CL2 * ((BSA/1.98)**0.75)* 39.7
&IF(CYP.EQ.1) CL =CL * CypCl
Q = Q0 * ((BSA/1.98)**0.75)* 39.7
V = V0 * (BSA/1.98)* 39.7
KE = CL/V
KCP = Q/V
KPC = Q/VP


Ka=Ka1
&IF(FORM.EQ.2) Ka = Ka2
```

```
#F
FA(1)= F2
&IF(TXT<14) FA(1) = F1
&IF(TXT>42) FA(1) = F3
&IF(FORM.EQ.2) FA(1) = FA(1) * Fadva
&IF(CYP.EQ.1) FA(1) = FA(1) * CypF

#LAG
TLAG(1)=Tlag2
&IF(TXT<14) TLAG(1) = Tlag1
&IF(TXT>42) TLAG(1) = Tlag3
&IF(FORM.EQ.2) TLAG(1) = TLAG(1) * TlagAdva

#OUT
F = X(2)/V
CU = F
BMAX = 4.18
KD = 3.8
CB = CU * HCT * BMAX / (CU + KD)

CONC = CU + CB

Y(1) = CONC


#ERR
G=10
0.2020500379, 0.0043193912, 0.0006024496,0
```

PRI, primary variables; Ka1, estimated absorptions rate constant for Prograf®; Ka2, estimated absorptions rate constant for Advagraf®; CL0, CL1, CL2, estimated values of clearance for different periods of time after transplantation; Q0, estimated intercompartmental clearance; V0, estimated volume of distribution; Vp0, estimated peripheral volume of distribution; Tlag1, Tlag2, Tlag3; estimated absorption lag times for three different periods of time after transplantation; TlagAdva, estimated absorption lag time for Advagraf®; F1, F2, F3, estimated values of bioavailability for three different periods of time after transplantation; Fadva, estimated value of bioavailability for Advagraf®; CypF, estimated effect of CYP3A5 genotype on bioavailability; CypCl, estimated effect of CYP3A5 genotype on clearance; COV, covariates; STU, the study the patient participated in identified by a number; STER, steroid dose in mg; M0F1, sex of the patient, 0=male, 1=female; WTKG, weight in kg; HT, height in cm; FFMES, fat-free mass in kg; TXT, time after transplantation in days; HCT, haematocrit; AGE, age in years; CYP, CYP3A5 genotype, 1=expressor of active CYP3A5, 0=non expressor; ASY, bioanalytical method; RICH, = rich data defined as 3 or more samples taken within the same dosing interval, 0=not rich data; EXACT: 1=the exact time for the previous tacrolimus dosing and the following blood samplings are known, 0=the exact time is unknown; FORM, type of tacrolimus formulation, 1=Prograf®, 2=Advagraf®; BMI, body mass index in kg/m2; BSA, body surface area in m2; SEC, secondary variables; CL, clearance; Q, intercompartmental clearance; V, volume of distribution; KE, elimination rate constant; KCP, transport rate constant from central compartment to peripheral compartment; KPC, transport rate constant from peripheral compartment back to central compartment; Ka, absorption rate constant; F, bioavailability; FA(1), bioavailability formula; LAG, lag time; TLAG, absorption lag time; OUT, outputs; CU, unbound tacrolimus concentration; BMAX, constant for tacrolimus binding to red blood cells; KD, association constant; CB, bound tacrolimus concentration; CONC, whole blood tacrolimus concentration; ERR, error; G, gamma.

Appendix C: Model file for the New model

```
#PRI
Ka1, 0.1, 4.5
Ka2, 0.1, 1.8
LAM, 0.1, 100
K14a, 0.001, 3.5
K15a, 0.01, 3.3
K23, 0.01, 5.0
K32, 0.001, 1.0
K20, 0.001, 1.5
V0, 10, 150
Tlag1a, 0.0, 6.0
Tlag1p, 0.0, 2.0
Tlag2a, 0.05, 2.5
Tlag3a, 0.05, 4.0
F1, 0.001, 1
Fadva, 0.001, 1
CypF, 0.05, 1.0
CypCl, 0.001, 2.2

#COV
IC
STU
STER
M0F1
WTKG
HT
FFMES
TXT
HCT
AGE
CYP
ASY
FORM
BMI
BSA
TDOSE

#SEC
V = V0  * (BSA/1.98)* 39.7
Ka=Ka1
&IF(FORM.EQ.2) Ka = Ka2
Pi = 3.1415927
Tlag1=Tlag1p
&IF(FORM.EQ.2) Tlag1=Tlag1a
K12 = Ka*(0.5*(1+ATAN(LAM*(T-TDOSE-Tlag1))*2/Pi))
K42 = Ka*(0.5*(1+ATAN(LAM*(T-TDOSE-Tlag2a))*2/Pi))
&IF(FORM.EQ.1) K42=0.D0
K52 = Ka*(0.5*(1+ATAN(LAM*(T-TDOSE-Tlag3a))*2/Pi))
&IF(FORM.EQ.1) K52=0.D0
K14=K14a
&IF(FORM.EQ.1) K14=0.D0
K15=K15a
&IF(FORM.EQ.1) K15=0.D0

#DIF
XP(1) = -(K12+K14+K15)*X(1)
XP(2) = K12*X(1) + K42*X(4) +K52*X(5) -
(K23+K20*EXP(CYP*CypCl))/((BSA/1.98)**0.25)*X(2) +
K32/((BSA/1.98)**0.25)*X(3)
XP(3) = K23/((BSA/1.98)**0.25)*X(2) - K32/((BSA/1.98)**0.25)*X(3)
XP(4) = K14*X(1) - K42*X(4)
XP(5) = K15*X(1) - K52*X(5)
```

```
#F
FA(1) = F1
&IF(FORM.EQ.2) FA(1) = Fadva
&IF(CYP.EQ.1) FA(1) = FA(1) * CypF

#INI
X(2) = 0.78*V*(IC*3.8)/(HCT*4.18-IC)
X(3) = V*(IC*3.8)/(HCT*4.18-IC)*(K23/K32)

#OUT
F = X(2)/V

CU = F
BMAX = 4.18
KD = 3.8
CB = CU * HCT * BMAX / (CU + KD)

CONC = CU + CB

Y(1)  = CONC


#ERR
L=5
0.2020500379, 0.0043193912, 0.0006024496,0
```

PRI, primary variables; Ka1, estimated absorptions rate constant for Prograf□; Ka2, estimated absorptions rate constant for Advagraf®; LAM, lambda used for the Heaviside step function; K14a, estimated transport rate constant from compartment 1 to 4 for Advagraf□; K15a, estimated transport rate constant from compartment 1 to 5 for Advagraf®; K23, estimated transport rate constant from compartment 2 to 3; K32, estimated transport rate constant from compartment 3 to 2; K20, estimated elimination rate constant; V0, estimated volume of distribution; Tlag1a, estimated absorption lag time for Advagraf® from compartment 1 to 2; Tlag1p, estimated absorption lag time for Prograf® for compartment 1 to 2; Tlag2a, estimated absorption lag time for Advagraf® for compartment 4 to 2; Tlag3a, estimated absorption lag time for Advagraf® for compartment 5 to 2; F1, estimated value of bioavailability for Prograf®; Fadva, estimated value of bioavailability for Advagraf®; CypF, estimated effect of CYP3A5 genotype on bioavailability; CypCl, estimated effect of CYP3A5 genotype on clearance; COV, covariates; IC, initial condition, equivalent to steady-state concentration; STU, the study the patient participated in identified by a number; STER, steroid dose in mg; M0F1, sex of the patient, 0=male, 1=female; WTKG, weight in kg; HT, height in cm; FFMES, fat-free mass in kg; TXT, time after transplantation in days; HCT, haematocrit; AGE, age in years; CYP, CYP3A5 genotype, 1=expressor of active CYP3A5, 0=non expressor; ASY, bioanalytical method; FORM, type of tacrolimus formulation, 1=Prograf®, 2=Advagraf®; BMI, body mass index in kg/m2; BSA, body surface area in m2; TDOSE, time of dose administration relative to first dose; SEC, secondary variables; V, volume of distribution; Ka, absorption rate constant; Tlag1, absorption lag time; K12, absorptions rate constant from compartment 1 to 2; K42, transport rate constant from compartment 4 to 2; K52, transport rate constant from compartment 5 to 2; K14, transport rate constant from compartment 1 to 4; K15, transport rate constant from compartment 1 to 5; DIF, Differential equations; XP(1), XP(2), XP(3), XP(4), XP(5) inputs and outputs of compartment 1, 2, 3, 4 and 5; F, bioavailability; FA(1), bioavailability formula; INI, initial conditions; X(2), X(3), amount in compartments 2 and 3 at time 0; OUT, outputs; CU, unbound tacrolimus concentration; BMAX, constant for tacrolimus binding to red blood cells; KD, association constant; CB, bound tacrolimus concentration; CONC, whole blood tacrolimus concentration; ERR, error; L, lambda.